

Instabilities of charged anti-de Sitter black holes

Takuya Katagiri* and Tomohiro Harada†

Department of Physics, Rikkyo University, Toshima, Tokyo 171-8501, Japan

(Dated: November 16, 2021)

Abstract

We study quasinormal frequencies (QNFs) $\omega = \omega_R + i\omega_I$ of scalar fields in the anti-de Sitter (AdS) spacetime and charged AdS black holes. We focus on some range of mass squared and adopt the Robin boundary condition parameterised by $\zeta \in [0, \pi]$ at the conformal infinity. In the AdS spacetime, there exists a critical value ζ_c such that there are only pure oscillations for $\zeta < \zeta_c$, while there is an exponentially growing mode for $\zeta > \zeta_c$. In the presence of black holes, the system of the neutral field has symmetry $\omega \rightarrow -\omega^*$, while it is deformed to $(\omega, eQ) \rightarrow (-\omega^*, -eQ)$ for the scalar field charge e and black hole charge Q . We further numerically study the first fundamental modes for black holes much smaller than the AdS length in 4 dimensions. For the neutral field, as ζ is increased from 0 to π , the QNF, initially with $\omega_I < 0$, moves towards the imaginary axis, and bifurcates into two with the same ω_R but different ω_I , both of which contact the imaginary axis, and finally the one goes up and the other down along the imaginary axis. The former passes the origin at $\zeta = \zeta_c$, so that the system becomes unstable. For the charged field, we have two physically different modes, the one with positive ω_R and the other negative. Due to superradiance, ζ_c becomes smaller than that for the neutral field. The mode with positive ω_R induces superradiant instability for $eQ > 0$, while the mode with negative ω_R does for $eQ < 0$. At $\zeta = \zeta_c$, this mode is purely oscillating. In the superradiance, the scalar field gains energy not from a black hole but from its ambient electric field, while the black hole gives its charge to the scalar field.

* katagiri@rikkyo.ac.jp

† harada@rikkyo.ac.jp

CONTENTS

I. Introduction	4
II. System and basic equations	5
III. Scalar field in the AdS spacetime	7
A. Brief review of exact results	7
B. Numerical investigation	9
IV. Neutral and charged scalar fields in AdS black holes	12
A. Field equations, boundary conditions, and symmetries	12
B. Matched asymptotic expansion for small AdS black holes	14
1. Near region: $r_+ < r \ll \ell$	14
2. Far region: $r_+ \ll r$	15
3. Matching in the overlapping region	16
V. Numerical results	17
A. Real part of QNFs	17
B. Stability of the scalar field	18
1. Neutral field	18
2. Charged field	19
C. Larger black hole	22
D. Fine structure	23
1. Neutral field	23
2. Charged field	24
3. Flow of QNFs with respect to ζ	25
VI. Physical interpretation	26
A. Electromagnetic superradiance	26
B. Particle picture	29
C. Thermodynamical insight	31
VII. Conclusion	32

Acknowledgments	34
A. Positive self-adjoint extension of symmetric operators	34
B. Validity of the matching of the near-region and far-region solutions	35
C. Asymptotic behaviours of the near-region and far-region solutions	37
D. Symmetry $(\omega, eQ) \rightarrow (-\omega^*, -eQ)$ in the matched asymptotic expansion	39
References	39

I. INTRODUCTION

The anti-de Sitter (AdS) spacetime is an exact solution of Einstein's field equations with a negative cosmological constant. The AdS spacetime is maximally symmetric and geodesically complete, while it fails to be globally hyperbolic. This means that we cannot uniquely predict the complete time development from the initial data on a spacelike hypersurface. Ref. [2] gives a method to define the initial value problem for a massless scalar field in static and non-globally hyperbolic spacetimes in terms of the self-adjoint extension. Ref. [1] discusses the same problem for scalar-vector-tensor linear perturbations in the AdS spacetime.

The stability of a spacetime is a fundamental and important problem. Usually, physically useful solutions are more or less stable. On the other hand, the onset of instability suggests the existence of a branch of solutions nonlinearly involving a stationary or oscillating perturbation. Therefore, the analysis of instability can lead to finding new solutions [3–6]. In the context of AdS/CFT correspondence [7], an asymptotically AdS black hole is dual to quantum field theory at finite temperature, and we can calculate the relaxation time of the dual theory from the decaying time scale of the perturbation on the AdS black hole spacetime. Also, its instability corresponds to the phase transition of the dual theory as seen in holographic superconductor [8–10]. Thus, we can see the phase structure of the (strongly coupled) quantum field theory in terms of higher-dimensional gravitational physics.

For an asymptotically flat rotating black hole, it is known that a bosonic wave scattered against the potential barrier of the black hole can be amplified. This process is called superradiance [11, 12]. Superradiance may cause the instability of the black hole in a confined system. This is called superradiant instability. The confined system is realised by the mass of a scalar field [13, 14] or the negative cosmological constant [15] or reflecting boundary conditions which guarantee no energy loss at a distant region from the black hole [16, 17]. Superradiance can occur around not only rotating black holes but also the Reissner-Nordström black hole [18]. For superradiance to occur in the Reissner-Nordström black hole, the scalar field needs to be charged. For a massless charged scalar field, superradiant instability of the asymptotically AdS charged black hole is discussed in [19, 20].

The other instability of the charged AdS black hole is known as near-horizon scalar condensation [8]. In the extremal limit, the black hole admits $AdS_2 \times S^2$ near the horizon. Then, the charged scalar field can effectively violate the 2-dimensional Breitenlohner and

Freedman bound [21, 22] near the black hole. That leads to the dynamical instability. This process also requires that the scalar field be charged.

In this paper, we analytically and numerically investigate quasinormal frequencies (QNFs) of neutral and charged massive scalar fields in the AdS spacetime and Reissner-Nordström-AdS black holes. In the latter case, to obtain the QNFs, we assume that black holes are much smaller than the AdS length scale. We then discuss the dynamical properties of the scalar field in terms of the QNFs. In Refs. [23, 24], similar discussions are presented for the Banados-Teitelboim-Zanelli spacetime.

This paper is organised as follows. In Section II, we introduce the system and the basic equations. In Section III, we briefly review Ref. [1] for a massive scalar field in the AdS spacetime and present a numerical result consistent with their result. In Section IV, we introduce symmetries in the QNFs and justify the matched asymptotic expansion method for the neutral and charged scalar fields in the charged small AdS black holes. In Section V, we show numerical results for QNFs for the neutral and charged scalar fields in the charged small AdS black hole. In Section VI, we give physical interpretation of the superradiant instability in the AdS black hole. In the final section, we summarise this paper. In the Appendix, we present mathematical notions, show the validity of the matching procedure in the matched asymptotic expansion, derive the asymptotic behaviours of the solutions, and explicitly confirm the symmetry in the QNFs. We adopt the sign convention and abstract index notation in Wald [33] and the unit in which $c = \hbar = 1$.

II. SYSTEM AND BASIC EQUATIONS

We consider the Einstein-Maxwell-scalar system with a negative cosmological constant. The action is given by

$$S = \int d^{d+2}x \sqrt{-g} \left[\frac{1}{16\pi} (R - 2\Lambda) + L_m + L_{em} \right] \quad (2.1)$$

with

$$L_m = - \left[(D_a \Psi) (D^a \Psi)^* + \xi R |\Psi|^2 + m_0^2 |\Psi|^2 \right], \quad (2.2)$$

$$L_{em} = - \frac{1}{16\pi} F_{ab} F^{ab}, \quad (2.3)$$

where R is the scalar curvature and $\Lambda (< 0)$ is the cosmological constant, $F_{ab} = \nabla_a A_b - \nabla_b A_a = \partial_a A_b - \partial_b A_a$ is the field strength, $D_a := \nabla_a - ieA_a$, ∇_a is the Levi-Civita covariant

derivative, A_a is a gauge field, e and m_0 are the charge and mass of the complex scalar field Ψ , respectively, and ξ is the nonminimal coupling constant to gravity. We assume $e \geq 0$ without loss of generality.

Varying Eq. (2.1) with respect to g_{ab} , we obtain Einstein's equations

$$G_{ab} + \Lambda g_{ab} = 8\pi T_{ab}, \quad (2.4)$$

where $T_{ab} = T_{(m)ab} + T_{(em)ab}$ with

$$T_{(m)ab} = [(D_a \Psi)(D_b \Psi)^* + (D_a \Psi)^*(D_b \Psi)] - g_{ab} [g^{cd}(D_c \Psi)(D_d \Psi)^* + \mu^2 \Psi \Psi^*], \quad (2.5)$$

$$T_{(em)ab} = \frac{1}{4\pi} \left(F_{ac} F_b{}^c - \frac{1}{4} g_{ab} F_{cd} F^{cd} \right) \quad (2.6)$$

with $\mu^2 \equiv m_0^2 + \xi R$ being the effective mass squared of the scalar field. μ^2 can be negative in the AdS spacetime. Varying Eq. (2.1) with respect to A_a , we obtain some components of Maxwell's equations

$$\nabla_b F^{ba} = -4\pi j_{(e)}^a, \quad (2.7)$$

where $j_{(e)}^a$ is the conserved electric current density given by

$$j_{(e)}^a = -ie [\Psi^*(D^a \Psi) - \Psi(D^a \Psi)^*]. \quad (2.8)$$

The rest of the components of Maxwell's equations

$$\nabla_{[a} F_{bc]} = 0 \quad (2.9)$$

are automatically satisfied by construction. Varying Eq. (2.1) with respect to Ψ , we obtain the equation of motion for Ψ

$$[(\nabla_a - ieA_a)(\nabla^a - ieA^a) - \mu^2] \Psi = 0. \quad (2.10)$$

From the above, we can find the conserved particle number current density j^a [33]:

$$j^a = -i[\Psi^*(D^a \Psi) - \Psi(D^a \Psi)^*]. \quad (2.11)$$

Since the electric current density $j_{(e)}^a$ is related to j^a through $j_{(e)}^a = ej^a$, we can identify the charge of the associated particle with e .

In the presence of the timelike Killing vector ξ^a , we can define the conserved energy current J^a as $J^a := -T_b^a \xi^b$, which can be decomposed as $J^a = J_{(m)}^a + J_{(em)}^a$, where $J_{(m)}^a := -T_{(m)b}^a \xi^b$ and $J_{(em)}^a := -T_{(em)b}^a \xi^b$.

We will focus on Eq. (2.10) regarding Ψ as a test field in the fixed spacetime and gauge field in Sections II–V. In Sections VI and VII, we will also discuss the other equations and the effect of the scalar field onto the spacetime and the gauge field.

III. SCALAR FIELD IN THE ADS SPACETIME

A. Brief review of exact results

We briefly review a neutral scalar field in the AdS spacetime based on Ishibashi and Wald [1]. From Eq. (2.10), the scalar field obeys the following equation:

$$(\nabla_\mu \nabla^\mu - \mu^2) \Psi = 0. \quad (3.1)$$

Since the AdS spacetime is static, Eq. (3.1) can be written in the form of

$$-\frac{\partial^2}{\partial t^2} \Psi = A \Psi, \quad (3.2)$$

where t is a Killing parameter and A is given by $A = -V D^i (V D_i) + \mu^2 V^2$, $V \equiv (-\xi^\mu \xi_\mu)^{1/2}$, $\xi^\mu = (\partial/\partial t)^\mu$ is a timelike Killing vector and D^i is the Levi-Civita covariant derivative on a constant t spacelike hypersurface.

Now we can view A as a linear operator $A : D \rightarrow K$, where D and K are the subspaces of the Hilbert space $\mathcal{H} = L^2$. The definitions of mathematical notions are given in Appendix A. If A in Eq. (3.2) is symmetric and positive, A has at least one self-adjoint extension A_E which is positive [32]. Moreover, if the boundary condition is specified, A_E is uniquely determined [25]. If we find a positive and unique A_E , we can define stable and unique evolution of Ψ from initial data [2]. Therefore, the problem of how to define stable and unique evolution in the non-globally hyperbolic (static) spacetime boils down to choose the boundary condition such that A_E is positive.

In the coordinates $(t, \chi, \theta^1, \theta^2, \dots, \theta^d)$, the metric of the unit $(d+2)$ -dimensional AdS spacetime is given by

$$ds^2 = \frac{\ell^2}{\sin^2 \chi} (-dt^2 + d\chi^2 + \cos^2 \chi d\Omega_d^2), \quad (3.3)$$

where $\chi \in [0, \pi/2]$ is a radial coordinate, $(\theta^1, \theta^2, \dots, \theta^d)$ correspond to angular coordinates, $d\Omega_d^2$ is the metric of the d dimensional sphere, and $\ell \equiv \sqrt{d(d+1)/(-2\Lambda)}$ is the AdS length scale. The origin is located at $\chi = \pi/2$, while $\chi = 0$ corresponds to the conformal infinity.

We assume that Ψ is in the form,

$$\Psi(t, \chi, \theta^1, \dots, \theta^d) = (\ell \cot \chi)^{-d/2} \psi(\chi) Y(\theta^1, \dots, \theta^d) e^{-i\omega t}, \quad (3.4)$$

where $Y_k(\theta^1, \dots, \theta^d)$ are spherical harmonics and $\omega \in \mathbb{C}$ is the frequency. Now Eq. (3.2) is rewritten as

$$A\psi(\chi) = \omega^2 \psi(\chi), \quad (3.5)$$

where

$$A = -\frac{d^2}{d\chi^2} + \frac{\nu^2 - 1/4}{\sin^2 \chi} + \frac{\rho^2 - 1/4}{\cos^2 \chi} \quad (3.6)$$

with $\nu^2 = 1/4 + d(d+2)/4 + \mu^2 \ell^2$ and $\rho^2 = 1/4 + l(l+d-1) + d(d-2)/4$. Note that A given by Eq. (3.6) is a symmetric operator.

We require that the general solution of Eq. (3.5) be regular at the origin. On the other hand, the asymptotic behaviour of the solution near the conformal infinity is given by

$$\psi(\chi) \sim C_1 \psi_{fast}(\chi) + C_2 \psi_{slow}(\chi), \quad C_1, C_2 \in \mathbb{C}, \quad (3.7)$$

where $\psi_{fast}(\chi)$ and $\psi_{slow}(\chi)$ show the faster and slower cutoffs in the limit to the conformal infinity $\chi \rightarrow 0$, respectively. In analogy, we refer to the boundary condition $C_2 = 0$ and $C_1 = 0$ as the Dirichlet and Neumann boundary conditions, respectively. Ref. [1] summarises the relation between the positivity of the self-adjoint extension of A and the boundary conditions at the conformal infinity as the following theorem.

Theorem 1: *Let A and A_E be the symmetric operator given by Eq. (3.6) and its self-adjoint extension, respectively. For the solution (3.7) which satisfies the regularity condition at the origin, the relation between the positivity of A_E and the boundary condition imposed at the conformal infinity is as follows:*

- (1) *If $-(d+3)(d-1)^2/4 \leq \mu^2 \ell^2$, there exists unique A_E , and it is positive.*
- (2) *If $-(d+1)^2/4 < \mu^2 \ell^2 < -(d+3)(d-1)^2/4$, A_E is positive if and only if*

$$\kappa \geq \kappa_c = - \left| \frac{\Gamma(-\nu)}{\Gamma(\nu)} \right| \frac{\Gamma(\zeta_{\nu,\rho}^0)^2}{\Gamma(\zeta_{-\nu,\rho}^0)^2}, \quad (3.8)$$

where $C_1 = \kappa C_2$ ($\kappa \in \mathbb{R}$), which is called the Robin boundary condition, and $\zeta_{\nu,\rho}^0 \equiv \nu + \rho + 1/2$.

- (3) *If $\mu^2 \ell^2 = -(d+1)^2/4$, A_E is positive if and only if $\kappa \leq \tilde{\kappa}_c = 2\gamma + 2P(\zeta_{0,\rho}^0)$, where $P(\zeta_{0,\rho}^0) \equiv d \log \Gamma(\chi)/d\chi|_{\chi=\zeta_{0,\rho}^0}$ and γ is the Euler number.*
- (4) *If $\mu^2 \ell^2 < -(d+1)^2/4$, A is unbounded below. Then, any A_E are unbounded below.*

B. Numerical investigation

Let us investigate the scalar field for the case **(2)** of this theorem. For this purpose, we shall solve Eq. (3.5) in the 4-dimensional AdS spacetime. Now we introduce a new variable

$$y = 1 + \frac{1}{\tan^2 \chi}, \quad (3.9)$$

and a function $g(y)$ such that

$$\psi(y) = y^{\frac{\omega\ell}{2}} (y-1)^{\frac{l}{2}} g(y). \quad (3.10)$$

Then Eq. (3.5) is reduced to an equation for $g(y)$,

$$y(1-y) \frac{d^2}{dy^2} g(y) + \{\gamma - (\alpha + \beta + 1)y\} \frac{d}{dy} g(y) - \alpha\beta g(y) = 0 \quad (3.11)$$

with

$$\begin{aligned} \alpha &= \frac{\omega\ell}{2} + \frac{l}{2} + \frac{3}{4} + \frac{1}{4} \sqrt{9 + 4\mu^2 \ell^2}, \\ \beta &= \frac{\omega\ell}{2} + \frac{l}{2} + \frac{3}{4} - \frac{1}{4} \sqrt{9 + 4\mu^2 \ell^2}, \\ \gamma &= \omega\ell + 1. \end{aligned} \quad (3.12)$$

Eq. (3.11) has two independent solutions

$$g(y) = y^{-\alpha} F\left(\alpha, \alpha - \gamma + 1; \alpha - \beta + 1; \frac{1}{y}\right), \quad y^{-\beta} F\left(\beta, \beta - \gamma + 1; \beta - \alpha + 1; \frac{1}{y}\right), \quad (3.13)$$

where $F(\ , \ ; \ ; \frac{1}{y})$ is the Gaussian hypergeometric function. We thus obtain the general solution of Eq. (3.5),

$$\begin{aligned} \psi(y) &= C y^{-\frac{l}{2} - \frac{3}{4} - \frac{1}{4} \sqrt{9 + 4\mu^2 \ell^2}} (y-1)^{\frac{l}{2}} F\left(\alpha, \alpha - \gamma + 1; \alpha - \beta + 1; \frac{1}{y}\right) \\ &\quad + D y^{-\frac{l}{2} - \frac{3}{4} + \frac{1}{4} \sqrt{9 + 4\mu^2 \ell^2}} (y-1)^{\frac{l}{2}} F\left(\beta, \beta - \gamma + 1; \beta - \alpha + 1; \frac{1}{y}\right), \end{aligned} \quad (3.14)$$

where C and D are arbitrary constants in \mathbb{C} .

Near the conformal infinity, Eq. (3.14) behaves as

$$\psi(\chi) \sim C \chi^{\frac{3}{2} + \frac{1}{2} \sqrt{9 + 4\mu^2 \ell^2}} + D \chi^{\frac{3}{2} - \frac{1}{2} \sqrt{9 + 4\mu^2 \ell^2}}. \quad (3.15)$$

This is an explicit form of Eq. (3.7). According to Theorem 1, we have a degree of freedom in choosing the boundary condition depending on the value of $\mu^2 \ell^2$. We here focus on the case $-9/4 < \mu^2 \ell^2 < -5/4$ and impose the Robin boundary condition

$$C = \kappa D, \quad \kappa \in \mathbb{R} \quad (3.16)$$

on Eq. (3.15). Then, the AdS spacetime behaves as a confined system because Eq. (3.16) gives a reflecting boundary condition [24]. In the context of AdS/CFT correspondence, this boundary condition corresponds to the double-trace deformation and the one parameter of the boundary condition determines its coupling constant [26]. We thus obtain the solution of Eq. (3.5) satisfying the boundary condition at the conformal infinity as follows:

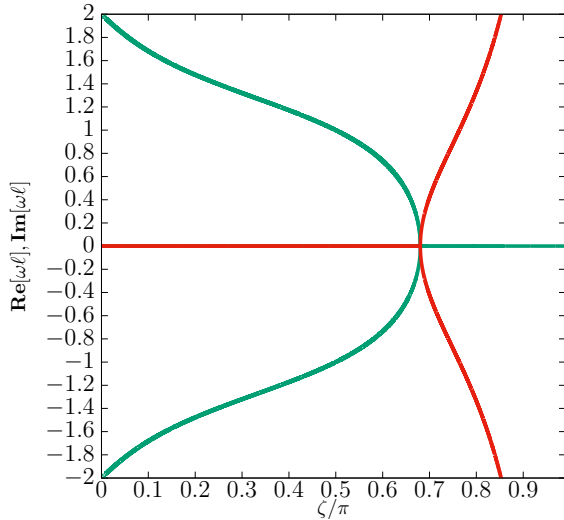
$$\psi(y) = D \left[\kappa y^{-\frac{l}{2}-\frac{3}{4}-\frac{1}{4}\sqrt{9+4\mu^2\ell^2}} (y-1)^{\frac{l}{2}} F\left(\alpha, \alpha-\gamma+1; \alpha-\beta+1; \frac{1}{y}\right) + y^{-\frac{l}{2}-\frac{3}{4}+\frac{1}{4}\sqrt{9+4\mu^2\ell^2}} (y-1)^{\frac{l}{2}} F\left(\beta, \beta-\gamma+1; \beta-\alpha+1; \frac{1}{y}\right) \right]. \quad (3.17)$$

As shown in Appendix C, in the limit of $y \rightarrow 1$, or $\chi \rightarrow \pi/2$, Eq. (3.17) behaves as

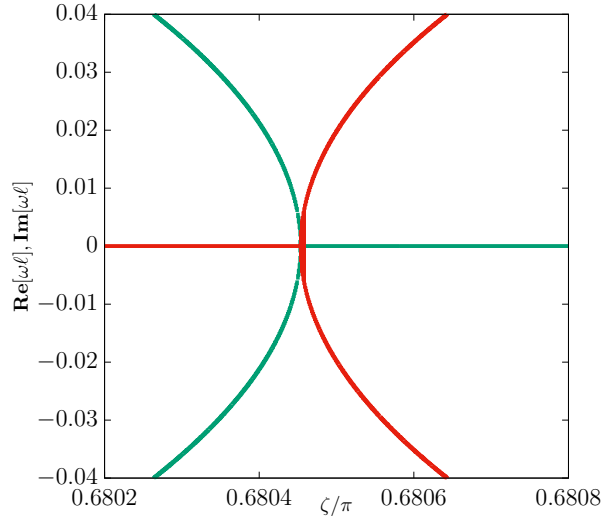
$$\psi(y) \sim D\Gamma(\alpha+\beta-\gamma) \left[D_1(\tilde{\omega}, \kappa) \left(\frac{\pi}{2} - \chi\right)^{-l-1} + D_2(\tilde{\omega}, \kappa) \left(\frac{\pi}{2} - \chi\right)^l \right], \quad (3.18)$$

where

$$\begin{aligned} D_1(\omega, \kappa) &= \frac{\kappa\Gamma(\alpha-\beta+1)}{\Gamma(\alpha)\Gamma(\alpha-\gamma+1)} + \frac{\Gamma(\beta-\alpha+1)}{\Gamma(\beta)\Gamma(\beta-\gamma+1)}, \\ D_2(\omega, \kappa) &= \frac{\Gamma(\gamma-\alpha-\beta)}{\Gamma(\alpha+\beta-\gamma)} \left(\frac{\kappa\Gamma(\alpha-\beta+1)}{\Gamma(1-\beta)\Gamma(\gamma-\beta)} + \frac{\Gamma(\beta-\alpha+1)}{\Gamma(1-\alpha)\Gamma(\gamma-\alpha)} \right). \end{aligned} \quad (3.19)$$



(a) The relation between ζ and ω .



(b) The enlarged figure of Figure 1(a).

Figure 1. The relation between ζ and ω of QNFs with $d = 2$, $l = 0$, and $\mu^2\ell^2 = -2$. The real and imaginary parts of ω are denoted by green and red lines, respectively.

We can see that the first term in the square brackets on the right-hand side of Eq. (3.18) diverges at $\chi = \pi/2$ if $D_1(\omega, \kappa) \neq 0$. Therefore, to guarantee the regularity at the origin, we

require

$$D_1(\omega, \kappa) = 0. \quad (3.20)$$

This equation determines the eigenfrequency or the QNF of the mode which satisfies the boundary condition. It also gives us the relation between the evolution and the boundary condition at the conformal infinity. Here we can see that the functions $D_1(\omega, \kappa)$ and $D_2(\omega, \kappa)$ have a symmetry under the transformation $\omega \rightarrow -\omega$, and moreover satisfy the relation $D_1(\omega, \kappa) = D_1^*(-\omega^*, \kappa)$ and $D_2(\omega, \kappa) = D_2^*(-\omega^*, \kappa)$. Thus, if ω is a QNF, then, both of $-\omega$ and $-\omega^*$ and therefore ω^* are.

Now we redefine the parameter of the boundary condition as $\zeta \equiv \text{ArcTan}[1/\kappa] \in (0, \pi)$, where ζ is a monotonically decreasing function of $\kappa \in \mathbb{R}$ with $\zeta = 0$ and $\zeta = \pi/2$ corresponding to the Dirichlet and Neumann conditions, respectively. Then the stability criterion $\kappa \geq \kappa_c$ corresponds to $\zeta \leq \zeta_c$ in terms of ζ , where we have defined

$$\zeta_c \equiv \text{ArcTan} \left[- \left| \frac{\Gamma(\nu)}{\Gamma(-\nu)} \right| \frac{\Gamma(\zeta_{-\nu, \rho}^0)^2}{\Gamma(\zeta_{\nu, \rho}^0)^2} \right]. \quad (3.21)$$

For s-wave ($l = 0$) in the 4-dimensional AdS spacetime, substituting $d = 2$, $\mu^2 \ell^2 = -2$, and $l = 0$, we find

$$\zeta_c \simeq 0.68045\pi. \quad (3.22)$$

We numerically solve Eq. (3.20) by the Newton-Raphson method. Figures 1(a) and 1(b) present the relation between ζ and ω . Here we choose $d = 2$, $l = 0$, and $\mu^2 \ell^2 = -2$. The vertical axis denotes $\text{Re}[\omega \ell]$ and $\text{Im}[\omega \ell]$. The horizontal axis denotes the normalised parameter ζ/π . The green and red lines denote $\text{Re}[\omega \ell]$ and $\text{Im}[\omega \ell]$, respectively. Figure 1(b) is the enlarged figure of Figure 1(a) in the region given by $\text{Re}[\omega \ell], \text{Im}[\omega \ell] \in [-0.04, 0.04]$ and $\zeta/\pi \in [0.6802, 0.6808]$. These figures show that $\text{Re}[\omega \ell]$ decreases as ζ increases for $\zeta \leq \zeta_c \simeq 0.68\pi$ and $\text{Re}[\omega \ell] = 0$ for $\zeta_c < \zeta$. We can also see that $\text{Im}[\omega \ell]$ is zero for $\zeta \leq \zeta_c$, while it takes two values, the one is positive and the other negative with the same absolute value for $\zeta_c < \zeta$. Hence, the operator A of Eq. (3.5) fails to be positive for $\zeta_c < \zeta$ because there is a mode of which the imaginary part of frequency is positive. This means that the mode is unstable for $\zeta_c < \zeta$ or $\kappa < \kappa_c$.

IV. NEUTRAL AND CHARGED SCALAR FIELDS IN ADS BLACK HOLES

A. Field equations, boundary conditions, and symmetries

Using the Schwarzschild-like coordinates (t, r, θ, ϕ) , the line element in the Reissner-Nordström-AdS spacetime in 4 dimensions is written in the form

$$ds^2 = -\frac{\Delta}{r^2} dt^2 + \frac{r^2}{\Delta} dr^2 + r^2 (d\theta^2 + \sin^2 \theta d\phi^2) \quad (4.1)$$

with

$$\Delta := r^2 - 2Mr + Q^2 + \frac{r^4}{\ell^2} = (r - r_+)(r - r_-)R(r), \quad (4.2)$$

$$R(r) := 1 + \left(\frac{r}{\ell}\right)^2 + \left(\frac{r_+}{\ell} + \frac{r_-}{\ell}\right) \left(\frac{r}{\ell}\right) + \left(\frac{r_+}{\ell}\right)^2 + \left(\frac{r_-}{\ell}\right)^2 + \left(\frac{r_+}{\ell}\right) \left(\frac{r_-}{\ell}\right), \quad (4.3)$$

where M is the mass and Q is the charge of the black hole. There are two Killing horizons located at $r = r_+$ and $r = r_-$ ($0 < r_- < r_+$). We call $r = r_+$ and $r = r_-$ outer and inner horizons, respectively. The black hole is the region given by $r < r_+$. Hereafter, we will consider the evolution of the scalar field in the region $r_+ < r$.

The equation of motion for the scalar field is given by Eq. (2.10) with the 1-form of the gauge field given by

$$A_\mu dx^\mu = -\left(\frac{Q}{r} + \phi_0\right) dt, \quad (4.4)$$

where $\phi_0 \in \mathbb{R}$ is an integration constant. Since the spacetime is static and spherically symmetric, we can expand Ψ in terms of spherical harmonics $Y_{lm}(\theta, \phi)$ as

$$\Psi(t, r, \theta, \phi) = \sum_{l,m} \frac{u_{lm}(r)}{r} Y_{lm}(\theta, \phi) e^{-i\omega_{lm}t}, \quad (4.5)$$

where $\omega_{lm} \in \mathbb{R}$ is the frequency. Note that the above sign convention is naturally consistent with that for the gauge covariant derivative. Hereafter, we focus on a single set of (l, m) and just write $u_{lm}(r)$ and ω_{lm} as $u(r)$ and ω , respectively.

Since we discuss the dynamical properties of a scalar field in Eq. (4.1) in terms of quasinormal modes, we now assume $\omega \in \mathbb{C}$. Redefining the radial part by $\psi(r) = u(r)/r$, Eq. (2.10) can be written in the form

$$\left[\frac{d}{dr} \left(\Delta \frac{d}{dr} \right) + \frac{r^4}{\Delta} \left(\tilde{\omega} - \frac{eQ}{r} \right)^2 - l(l+1) - \mu^2 r^2 \right] \psi(r) = 0, \quad (4.6)$$

where $\tilde{\omega} := \omega - e\phi_0$.

Introducing the tortoise coordinate x by

$$dx = \frac{r^2}{\Delta} dr, \quad x \in (-\infty, +\infty), \quad (4.7)$$

in the limit $x \rightarrow -\infty$ or to the outer horizon, Eq. (4.6) becomes

$$\left[\frac{d^2}{dx^2} + \left(\tilde{\omega} - \frac{eQ}{r_+} \right)^2 \right] \psi(x) \simeq 0, \quad (4.8)$$

and the general solution of Eq. (4.8) behaves as

$$\psi(x) \sim B_{\text{in}} e^{-i(\tilde{\omega} - \frac{eQ}{r_+})x} + B_{\text{out}} e^{i(\tilde{\omega} - \frac{eQ}{r_+})x}, \quad B_{\text{in}}, B_{\text{out}} \in \mathbb{C}. \quad (4.9)$$

Here the subscripts “in” and “out” denote the ingoing and outgoing modes at the outer horizon, respectively. We demand that $B_{\text{out}} = 0$ so that the ingoing-wave condition at the outer horizon can be satisfied.

As for the boundary condition at the conformal infinity, we expect that the classification of Theorem 1 does not change even in the presence of a black hole because that classification is based on the asymptotic behaviour of the field near the conformal infinity, although the critical values κ_c and $\tilde{\kappa}_c$ could change because the regularity condition at the origin is replaced with the ingoing-wave condition at the black hole horizon. If both the scalar field and the black hole are charged, there can also appear electromagnetic superradiant instability. The electromagnetic superradiance in the asymptotically flat charged black hole will be briefly reviewed in Section VI A. It should also be noted that the equation of motion for the charged scalar field cannot be written in the Schrödinger form as in Eq. (3.2). Hence, Theorem 1 does not apply for the charged scalar field.

We simultaneously demand the ingoing-wave condition $B_{\text{out}} = 0$ at the horizon and the Robin boundary condition (3.16) with the asymptotic form (3.15) at the conformal infinity. In general, this can be met only a discrete set of complex frequencies. These are called QNFs. Here it is useful to see what symmetry this system has. Eq. (4.6) trivially admits symmetry $(\omega, eQ, \psi) \rightarrow (-\omega, -eQ, \psi)$, while we can find other symmetries $(\omega, eQ, \psi) \rightarrow (\omega^*, eQ, \psi^*)$ and $(\omega, eQ, \psi) \rightarrow (-\omega^*, -eQ, \psi^*)$. Since $\kappa \in \mathbb{R}$ and the asymptotic form (3.15) does not depend on $\tilde{\omega}$, if the Robin boundary condition is satisfied by ψ , it is also by ψ^* . Therefore, all these three transformations are consistent with the Robin boundary condition at the conformal infinity. However, only the transformation $(\omega, eQ, \psi) \rightarrow (-\omega^*, -eQ, \psi^*)$ among

the three can satisfy the ingoing-wave condition at the outer horizon. Therefore, only this transformation remains as the symmetry of the system, which necessarily involves charge conjugation. In other words, $\omega \rightarrow -\omega^*$ is no longer the symmetry of the system for the charged scalar field if we fix eQ .

B. Matched asymptotic expansion for small AdS black holes

To treat Eq. (4.6) analytically, we apply the matched asymptotic expansion method. The strategy is as follows. We first assume $-9/4 < \mu^2 \ell^2 < -5/4$, for which the Robin boundary condition applies. We also assume that the black hole radius is much smaller than the AdS length scale: $r_+ \ll \ell$. Then, we consider two spatial regions outside the black hole. We call the regions given by $r_+ < r \ll \ell$ and $r_+ \ll r$ near and far regions, respectively. Then, we obtain an approximate analytic solution which satisfies the imposed boundary condition in each region. We will show that the two regions have an overlapping region satisfying $r_+ \ll r \ll \ell$, where the both approximate solutions are valid. Then, we match the two solutions there and the matching condition gives an eigenvalue equation for the frequency. Thus, we obtain QNFs and the approximate analytic solution which satisfies the boundary conditions both at the horizon and at the conformal infinity.

1. Near region: $r_+ < r \ll \ell$

In the near region, since $\Delta \simeq (r - r_+)(r - r_-)$, the metric is approximated by the Reissner-Nordström metric. Now we introduce a new coordinate,

$$z = \frac{r - r_+}{r - r_-}, \quad (4.10)$$

and a function $f(z)$ such that

$$\psi(z) = z^{i\sigma} (1 - z)^{l+1} f(z), \quad (4.11)$$

where

$$\sigma = \frac{\left(\tilde{\omega} - \frac{eQ}{r_+}\right) r_+^2}{r_+ - r_-}. \quad (4.12)$$

Then Eq. (4.6) is reduced to

$$z(1 - z) \frac{d^2}{dz^2} f(z) + \{c - (a + b + 1)z\} \frac{d}{dz} f(z) - (ab + \mathcal{E}_1(r)) f(z) = 0 \quad (4.13)$$

with

$$a = 2i\sigma + l + 1, b = l + 1, c = 2i\sigma + 1, \quad (4.14)$$

and

$$\mathcal{E}_1(r) := \mu^2 r^2 \left(\frac{r - r_-}{r_+ - r_-} \right) + \frac{1}{(r_+ - r_-)(r - r_+)} \left\{ r_+^4 \left(\tilde{\omega} - \frac{eQ}{r_+} \right)^2 - r^4 \left(\tilde{\omega} - \frac{eQ}{r} \right)^2 \right\}. \quad (4.15)$$

In Appendix B, it is shown that $\mathcal{E}_1(r) \ll 1$ in the near region.

The two independent solutions of Eq. (4.13) in the region $1 < x \leq x_0$ can be written in terms of the Gaussian hypergeometric functions $F(\cdot, \cdot; \cdot; z)$ as

$$f(z) = F(a, b; c; z), \quad z^{1-c} F(1 - c + a, 1 - c + b; 2 - c; z). \quad (4.16)$$

We thus obtain the general solution of Eq. (4.6) in the region $x \leq x_0$,

$$\psi(z) = Az^{i\sigma}(1 - z)^{l+1}F(a, b; c; z) + Bz^{-i\sigma}(1 - z)^{l+1}F(1 - c + a, 1 - c + b; 2 - c; z), \quad (4.17)$$

where A and B are arbitrary constants. The first and second terms on the right-hand side are the outgoing and ingoing modes, respectively. Now we impose the ingoing-wave condition on Eq. (4.17), so that the first term should vanish. Thus, we obtain the following approximate analytic solution in the region $x \leq x_0$:

$$\psi(z) = Bz^{-i\sigma}(1 - z)^{l+1}F(1 - c + a, 1 - c + b; 2 - c; z). \quad (4.18)$$

2. Far region: $r_+ \ll r$

In the far region, since $\Delta \simeq r^2(1 + r^2/\ell^2)$, the metric is approximated by the AdS metric. Using a new variable

$$y = 1 + \frac{r^2}{\ell^2}, \quad (4.19)$$

which is equivalent to Eq. (3.9), and Eq. (3.10) with the replacement of ω with $\tilde{\omega}$, Eq. (4.6) is reduced to the equation for $g(y)$ given by

$$y(1 - y) \frac{d^2}{dy^2} g(y) + \{\gamma - (\alpha + \beta + 1)y\} \frac{d}{dy} g(y) - (\alpha\beta + \mathcal{E}_2(r)) g(y) = 0, \quad (4.20)$$

where α, β , and γ are defined by Eq. (3.12) with the replacement of ω with $\tilde{\omega}$ and

$$\mathcal{E}_2(r) := \frac{1}{4} (eQ) \left(\frac{r}{\ell} \right)^{-1} \left(1 + \frac{r^2}{\ell^2} \right)^{-1} \left\{ 2(\tilde{\omega}\ell) - (eQ) \left(\frac{r}{\ell} \right)^{-1} \right\}. \quad (4.21)$$

In Appendix B, it is shown that $|\mathcal{E}_2(r)| \ll 1$ in the far region.

Near the conformal infinity, the scalar field behaves as

$$\psi(r) \sim C \left(\frac{r}{\ell}\right)^{-\frac{3}{2}-\frac{1}{2}\sqrt{9+4\mu^2\ell^2}} + D \left(\frac{r}{\ell}\right)^{-\frac{3}{2}+\frac{1}{2}\sqrt{9+4\mu^2\ell^2}}, \quad (4.22)$$

where C and D are arbitrary constants. Since we have assumed $-9/4 < \mu^2\ell^2 < -5/4$, we impose the Robin boundary condition Eq. (3.16). Thus, we find Eq. (3.17) with the replacement of ω by $\tilde{\omega}$ as an approximate solution in the far region.

3. Matching in the overlapping region

Next we match the near-region and far-region approximate solutions, given by Eqs. (4.18) and (3.17), respectively, in the overlapping region. In Appendix B, we show that there really exists an overlapping region, where both the near-region and far-region approximate solutions are valid, if $\tilde{\omega}\ell = O(1)$ and $eQ = o(\epsilon^{1/3+\delta})$ with $\epsilon = r_+/\ell$ and $0 < \delta < 2/3$. We consider the asymptotic behaviour of them there. First, we see the asymptotic behaviour of the near-region solution (4.18) at $z \sim 1$. As shown in Appendix C, in the limit of $z \rightarrow 1$, Eq. (4.18) behaves as

$$\psi(z) \sim B\Gamma(1-2i\sigma) [B_1(\tilde{\omega}, \sigma)r^{-l-1} + B_2(\tilde{\omega}, \sigma)r^l], \quad (4.23)$$

where

$$B_1(\tilde{\omega}, \sigma) = \frac{\Gamma(-2l-1)(r_+ - r_-)^{l+1}}{\Gamma(-2i\sigma - l)\Gamma(-l)}, \quad B_2(\tilde{\omega}, \sigma) = \frac{\Gamma(2l+1)(r_+ - r_-)^{-l}}{\Gamma(-2i\sigma + l + 1)\Gamma(l+1)}. \quad (4.24)$$

Note that the functions $B_1(\tilde{\omega}, \sigma)$ and $B_2(\tilde{\omega}, \sigma)$ satisfy the relation $B_1(\tilde{\omega}, \sigma) = B_1^*(-\tilde{\omega}^*, -\sigma^*)$ and $B_2(\tilde{\omega}, \sigma) = B_2^*(-\tilde{\omega}^*, -\sigma^*)$, respectively.

Next, as derived in Appendix C, in the limit of $y \rightarrow 1$, the asymptotic form of the far-region solution (3.17) is given by Eq. (3.18). Using $r = 1/\tan \chi$, we find that Eq. (3.18) has the same form as Eq. (4.23).

Since both $y \sim 1$ and $z \sim 1$ are satisfied for $x_1 < x < x_0$, we can match Eq. (4.23) and Eq. (3.18) and obtain

$$\frac{B_1(\tilde{\omega}, \sigma)}{B_2(\tilde{\omega}, \sigma)} = \ell^{2l+1} \frac{D_1(\tilde{\omega}, \kappa)}{D_2(\tilde{\omega}, \kappa)}, \quad (4.25)$$

where $D_1(\tilde{\omega}, \kappa)$ and $D_2(\tilde{\omega}, \kappa)$ are defined by Eq. (3.19). The above gives the relation between κ and $\tilde{\omega}$. It is shown in Appendix D that the above equation is consistent with the symmetry $(\omega, eQ) \rightarrow (-\omega^*, -eQ)$.

V. NUMERICAL RESULTS

We numerically solve Eq. (4.25) by the Newton-Raphson method. We present the result in this section. Hereafter, we fix the mass parameter $\mu^2\ell^2 = -2$ and focus the s-wave, i.e., $l = 0$.

A. Real part of QNFs

Figures 2(a) and 2(b) give the relation between ζ and $\text{Re}[\omega] \geq 0$ for the neutral field in the AdS black hole with $(r_+, r_-) = (0.01\ell, 0.001\ell)$ and the AdS spacetime, respectively. The vertical and horizontal axes denote $\text{Re}[\omega\ell]$ and the normalised parameter ζ/π , respectively. The symmetry $\omega \rightarrow -\omega$ implies that the whole graph has reflectional symmetry with respect to the line $\text{Re}[\omega\ell] = 0$.

We note that only the result for the neutral field is plotted since the results for the neutral and charged fields are indistinguishable in this plot with this parameter set. We call the modes with the smallest and second smallest real parts of frequency first and second fundamental modes, respectively. On the first fundamental mode of the AdS black hole, we stop the numerical calculation at $\zeta = 0.88\pi$, above which the numerical error becomes large. The results for the second fundamental mode are plotted in the whole region $0 \leq \zeta \leq \pi$ for both cases.

Figures 2(a) and 2(b) show that the real part of the QNF of the neutral field in the AdS black hole has the same behaviour as in the AdS spacetime qualitatively. Namely, $|\text{Re}[\omega]|$ of the second fundamental mode decreases as ζ increases, and moreover $|\text{Re}[\omega]|$ of the first fundamental mode decreases as ζ increases for $\zeta \leq \zeta_0 \simeq 0.68\pi$ but becomes zero for $\zeta_c \leq \zeta$. The detailed result of the first fundamental mode near $\zeta = 0.68\pi$ is shown in Figures 3(a) and 3(b).

Hereafter we focus on the first fundamental mode because it is most relevant to the stability of the system. Figures 3(a) and 3(b) show the relation between ζ and $\text{Re}[\tilde{\omega}\ell]$ for the charged fields in the AdS black hole with $(r_+, r_-) = (0.01\ell, 0.001\ell)$. The green, purple, red, and blue lines denote the result with $eQ = 0, 0.01, 0.02$, and 0.03 , respectively. We stress that they are not the reflection of each other with respect to the line $\text{Re}[\omega] = 0$ because the symmetry of the system is deformed to $(\tilde{\omega}, eQ) \rightarrow (-\tilde{\omega}^*, -eQ)$ as stated in Section IV A.

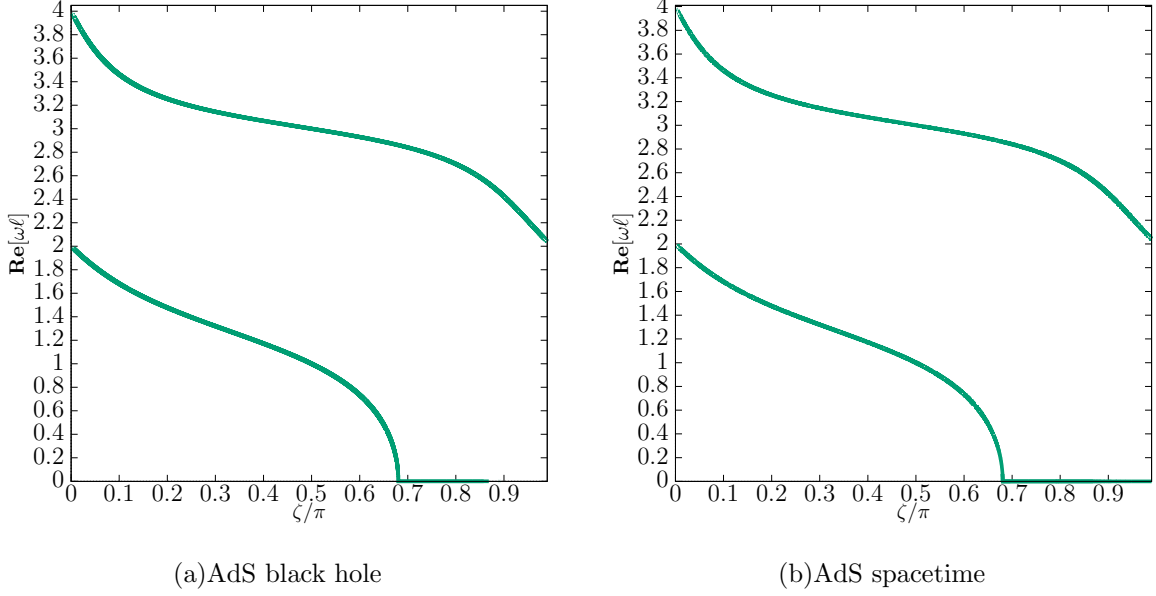


Figure 2. The relation between ζ and $\text{Re}[\omega\ell] \geq 0$ for the neutral field in the AdS black hole with $(r_+, r_-) = (0.01\ell, 0.001\ell)$ and the AdS spacetime.

However, since the result for the negative eQ is not distinguishable from that for the positive eQ of the same absolute value in this plot, we plot the result only for the positive eQ . As we will see later, they can be distinguishable for a larger black hole. We can also see that the neutral field has a critical value $\zeta_0 \simeq 0.68\pi$ at which $\text{Re}[\omega]$ becomes zero within the numerical error, while the charged field does not. For this reason, we define the critical value ζ_0 only for the neutral field, while the charged field does not have such a critical value.

B. Stability of the scalar field

We judge stability of the scalar field by the sign of the imaginary part of the QNF. If the imaginary part is positive, the mode is unstable.

1. Neutral field

Figures 4(a) and 4(b) give the relation between ζ and $\text{Im}[\omega]$ for the neutral field in the AdS black hole with $(r_+, r_-) = (0.01\ell, 0.001\ell)$. The imaginary parts of the both modes with positive and negative real parts give the same value because of the symmetry $\omega \rightarrow -\omega^*$ as stated in Section IV A. Figure 4(a) shows that the positive $\text{Im}[\omega]$ appears for $\zeta_c < \zeta$, where

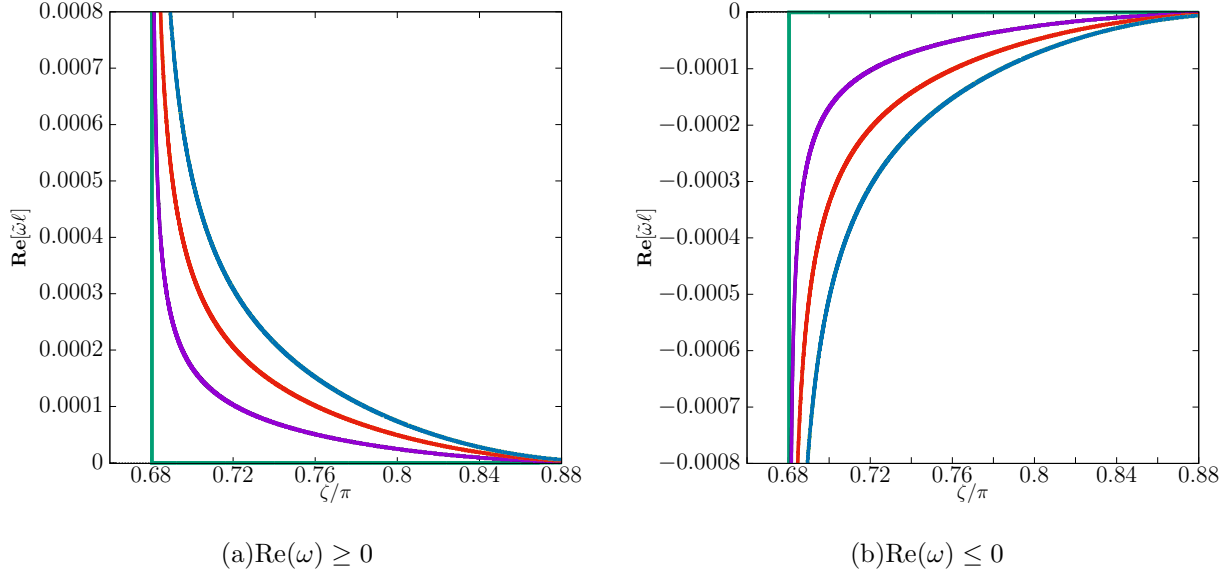
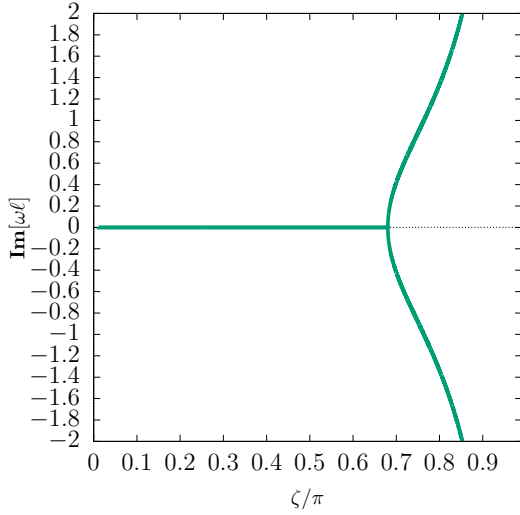


Figure 3. Same as Figure 2(a) but magnified near $\zeta = 0.68\pi$ for the neutral and charged fields in the AdS black hole with $(r_+, r_-) = (0.01\ell, 0.001\ell)$. The green, purple, red, and blue lines correspond to the result with $eQ = 0, 0.01, 0.02$, and 0.03 , respectively.

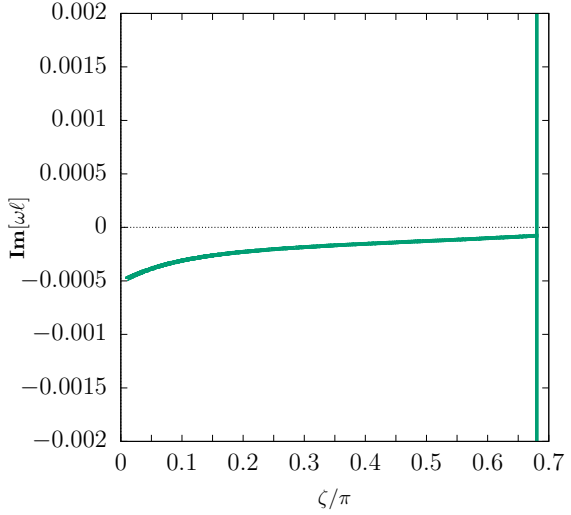
ζ_c is defined as the critical value at which there appears a mode with $\text{Im}[\omega] > 0$. It can be seen that $\text{Im}[\omega] < 0$ of the mode for $\zeta < \zeta_c$ and $\text{Im}[\omega] > 0$ for $\zeta > \zeta_c$. Furthermore, as we will see that $\zeta_0 < \zeta_c$ is satisfied. Figure 4(a) demonstrates that $\text{Im}[\omega]$ of the unstable mode increases as ζ increases. This instability is not due to superradiance but purely of boundary origin. Figure 4(b) is the enlarged figure of 4(a) in the range of $\zeta/\pi \in [0, 0.7]$, and $\text{Im}[\omega\ell] \in [-0.002, 0.002]$. This figure shows that the mode splits into two at $\zeta = \zeta_b < \zeta_c$.

2. Charged field

Figures 5(a) and 5(b) give the relation between ζ and $\text{Im}[\tilde{\omega}]$ for the mode with $\text{Re}[\tilde{\omega}] > 0$ for the charged field in the AdS black hole with $(r_+, r_-) = (0.01\ell, 0.001\ell)$. The yellow and blue lines denote the results with $eQ = 0.01$ and -0.01 , respectively. If we also plot curves for other positive values of eQ , they cannot be distinguished from that for $eQ = 0.01$ in this scale, and this is also the case for the negative values of eQ . Therefore, we plot only for the mode with $eQ = -0.01$ and 0.01 . Figures 5(a) and 5(b) show that if $eQ > 0$, there appears an unstable mode with $\text{Re}[\tilde{\omega}] > 0$ for $\zeta_c < \zeta$, where ζ_c is defined as the onset of instability also for the charged field. On the other hand, if $eQ < 0$, there appears an



(a) The relation between ζ and $\text{Im}(\omega\ell)$.

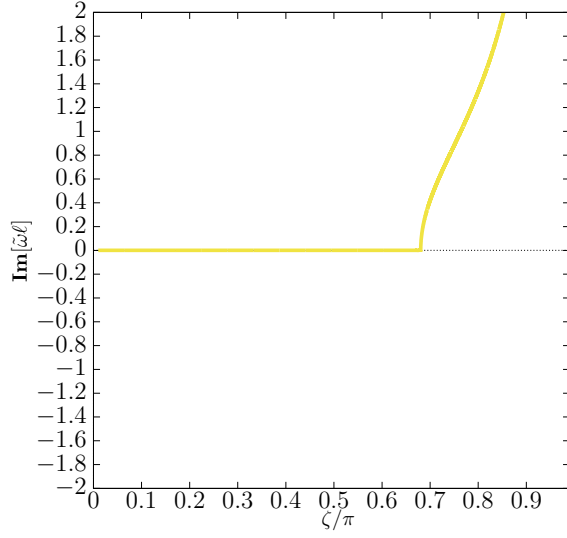


(b) The enlarged figure of Figure 4(a).

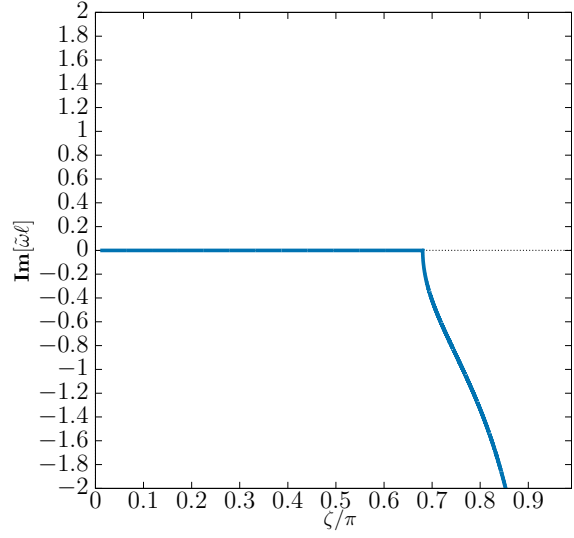
Figure 4. The relation between ζ and $\text{Im}[\omega\ell]$ for the neutral field in the AdS black hole with $(r_+, r_-) = (0.01\ell, 0.001\ell)$.

unstable mode with $\text{Re}[\tilde{\omega}] < 0$ for $\zeta_c < \zeta$. Note that the symmetry of the system is given by $(\tilde{\omega}, eQ) \rightarrow (-\tilde{\omega}^*, -eQ)$. We have checked that all of the unstable modes satisfy the superradiant condition Eq. (6.7) or (6.8), while none of the stable modes does. Hence, this instability comes from superradiance.

The detailed feature of the charged field for $\zeta \simeq \zeta_c$ is shown in Figures 6(a) and 6(b). They present the relation between ζ and $\text{Im}[\tilde{\omega}]$ for the charged field in the AdS black hole with $(r_+, r_-) = (0.01\ell, 0.001\ell)$. The results with $eQ = -0.01, 0.01, -0.02, 0.02, -0.03$, and 0.03 are denoted by the purple, black, red, orange, blue, and yellow lines, respectively. We can see that the mode with $\text{Re}[\tilde{\omega}\ell] > 0$ can be unstable for $eQ > 0$ even for $\zeta \leq \zeta_0$, while the mode with $\text{Re}[\tilde{\omega}\ell] < 0$ can be unstable for $eQ < 0$. As stated above, we have checked for any ζ we investigated that all of the unstable modes satisfy the superradiant condition Eq. (6.7) or (6.8), while none of the stable modes does. For this reason, we interpret that this instability arises from superradiance. Also, since the time scale of the instability for $\zeta_0 < \zeta$ can be much shorter than that for $\zeta \leq \zeta_0$, superradiant instability can be enhanced by the boundary condition.

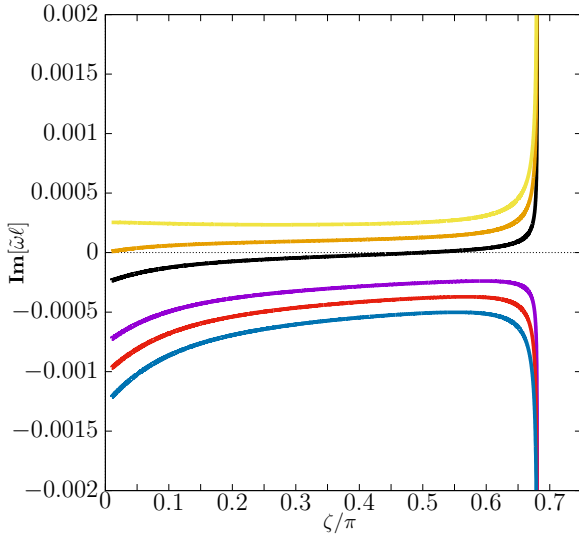


(a) $eQ = 0.01$

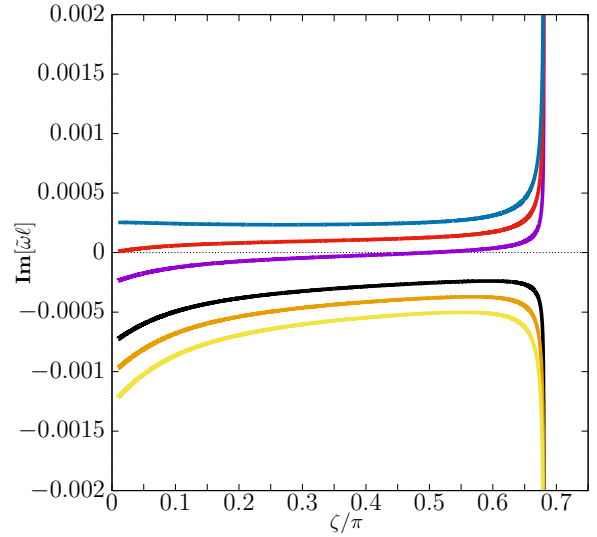


(b) $eQ = -0.01$

Figure 5. Same as Figure 4(a) for the mode with $\text{Re}[\tilde{\omega}] > 0$ for the charged field in the AdS black hole with $(r_+, r_-) = (0.01\ell, 0.001\ell)$. The yellow and blue lines denote $eQ = 0.01$ and -0.01 , respectively.



(a) $\text{Re}(\tilde{\omega}) > 0$



(b) $\text{Re}(\tilde{\omega}) < 0$

Figure 6. Same as Figure 4(b) but for the charged field in the AdS black hole with $(r_+, r_-) = (0.01\ell, 0.001\ell)$. The purple, black, red, orange, blue and yellow lines denote $eQ = -0.01, 0.01, -0.02, 0.02, -0.03$, and 0.03 , respectively.

C. Larger black hole

We investigate a black hole larger than the previous one. For this purpose, let us consider an AdS black hole with $(r_+, r_-) = (0.1\ell, 0.001\ell)$. Although it is not clear how much the condition Eq. (B5) is met, we would still continue to apply the matched asymptotic expansion method.

The relation between ζ and $\text{Re}[\tilde{\omega}]$ for the neutral and charged fields in the AdS black hole with $(r_+, r_-) = (0.1\ell, 0.001\ell)$ looks similar to Figures 3(a) and 3(b). However, there is a remarkable difference if it is magnified. Comparing Figures 7(a) and 7(b) with Figures 3(a) and 3(b), we can clearly see that the system does not have symmetry $(\omega, eQ) \rightarrow (-\omega^*, eQ)$ but $(\omega, eQ) \rightarrow (-\omega^*, -eQ)$.

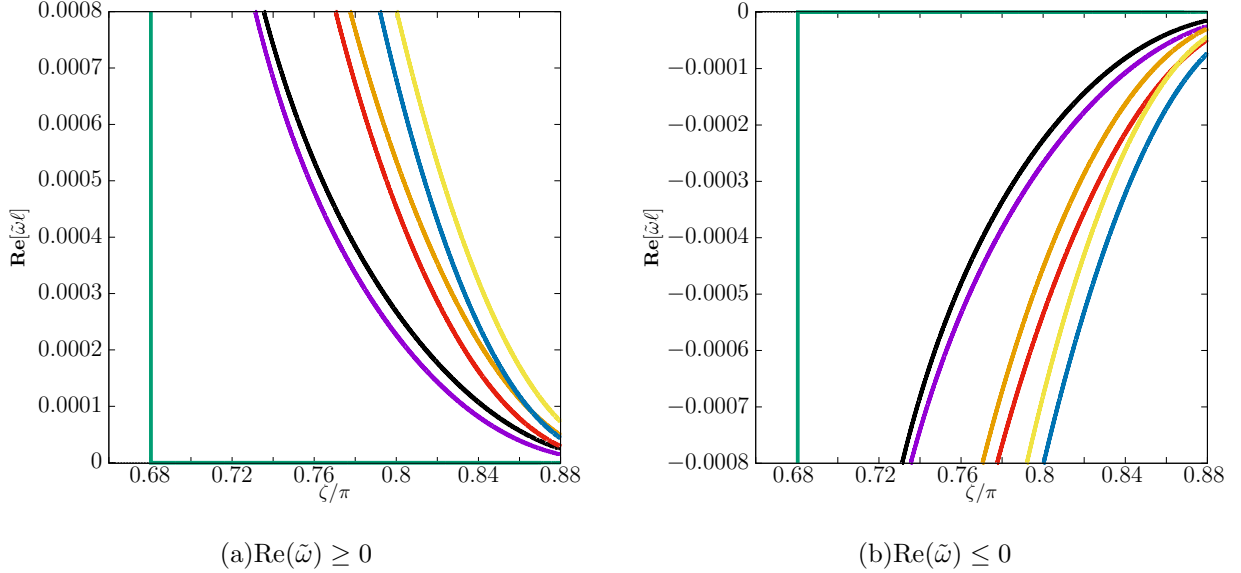


Figure 7. Same as Figures 3(a) and 3(b) but in the larger AdS black hole with $(r_+, r_-) = (0.1\ell, 0.001\ell)$. The green, purple, black, red, orange, blue, and yellow lines denote the results with $eQ = 0, -0.01, 0.01, -0.02, 0.02, -0.03$, and 0.03 ,

respectively.

Figures 8(a) and 8(b) give the relation between ζ and $\text{Im}[\tilde{\omega}]$ for the charged field in the AdS black hole with $(r_+, r_-) = (0.1\ell, 0.001\ell)$. The vertical and horizontal axes denote $\text{Im}[\tilde{\omega}\ell]$ and $\zeta/\pi \in [0, 0.7]$, respectively. Figures 8(a) and 8(b) show the similar behaviour to that seen in the smaller black hole with $(r_+, r_-) = (0.01\ell, 0.001\ell)$. Comparing these figures with Figures 4(b), 6(a), and 6(b), we can see that $|\text{Im}[\tilde{\omega}\ell]|$ of the stable mode for $\zeta \leq \zeta_0$ for the

AdS black hole with $(r_+, r_-) = (0.1\ell, 0.001\ell)$ are generally larger than those for the smaller black hole with $(r_+, r_-) = (0.01\ell, 0.001\ell)$ if we fix the values of ζ and eQ .

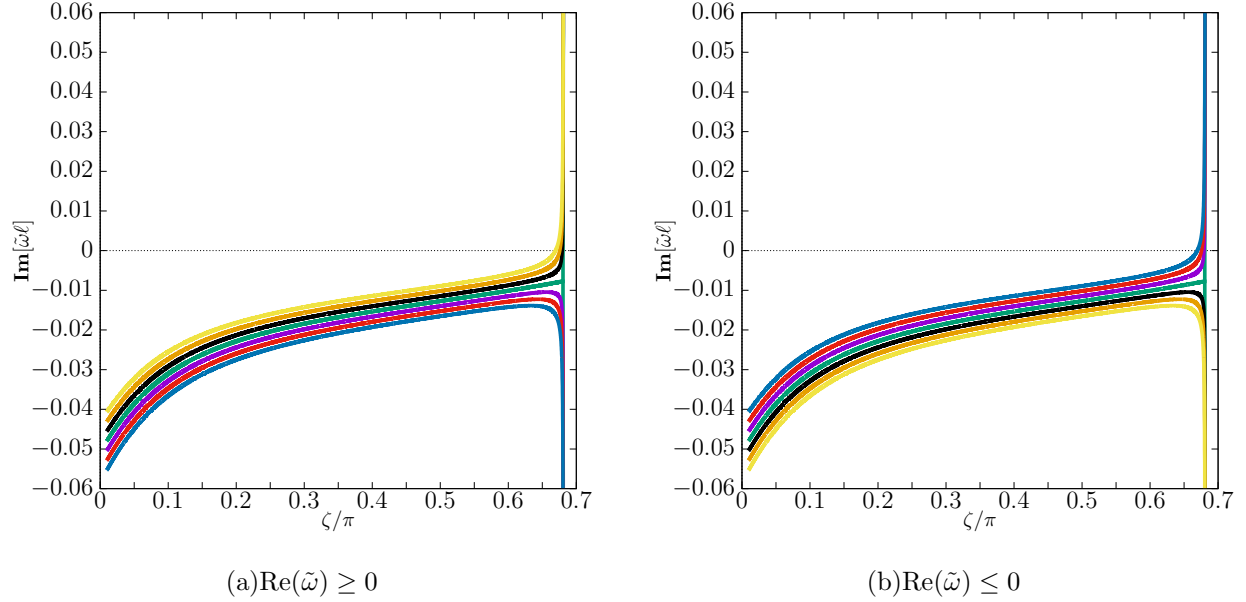


Figure 8. Same as Figure 4(b) but for the charged field in the larger AdS black hole with $(r_+, r_-) = (0.1\ell, 0.001\ell)$. The green, purple, black, red, orange, blue, and yellow lines denote the results with $eQ = 0, -0.01, 0.01, -0.02, 0.02, -0.03$ and 0.03 , respectively.

D. Fine structure

1. Neutral field

Here we shall discuss how the results for the neutral field in the AdS black hole are different from that in the AdS spacetime. Figure 9(a) gives the relation between ζ and $\omega\ell$ for the neutral field in the AdS black hole with $(r_+, r_-) = (0.1\ell, 0.001\ell)$ as in Figure 1(a). Figure 9(b) is the enlarged figure of Figure 9(a) in the range of $\zeta/\pi \in [0.68042, 0.68048]$ and $\text{Im}[\omega\ell] \in [-0.03, 0.03]$. Comparing these figures with Figures 1(a) and 1(b), we can see that the symmetries $\omega \rightarrow -\omega$ and $\omega \rightarrow \omega^*$ for the AdS spacetime are broken for the neutral field in the AdS black hole spacetime. Here we point out that the symmetry for the real part $\omega \rightarrow -\omega^*$ remains. Thus, a black hole breaks the symmetry. Physically, the negative imaginary part of the QNF for $\zeta \leq \zeta_c$ comes from the dissipation of the scalar field into the black hole.

Figure 9(b) shows that $\zeta_0 < \zeta_c$ is actually satisfied. It is also shown that $\zeta = \zeta_b$, which is defined as the bifurcation point at which the imaginary part splits into two different values, is slightly below ζ_0 . Hence, there are two QNFs which have one positive and one negative real parts of the same absolute value and the same negative imaginary part for $\zeta \leq \zeta_b$ but different negative imaginary parts for $\zeta_b < \zeta < \zeta_0$. Moreover, the two pure imaginary QNFs have one positive and one negative imaginary parts for $\zeta_c < \zeta$. Thus, we can see that there exists a static mode of the neutral field perturbation on the charged AdS black hole for $\zeta = \zeta_c$. This can be most clearly seen in Figure 11(a).

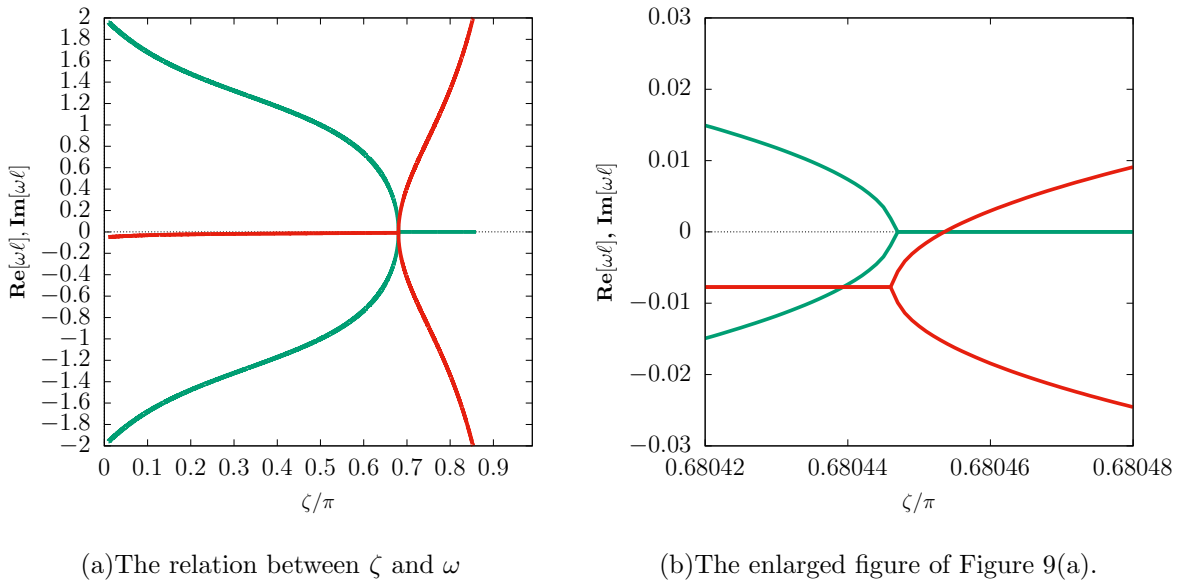
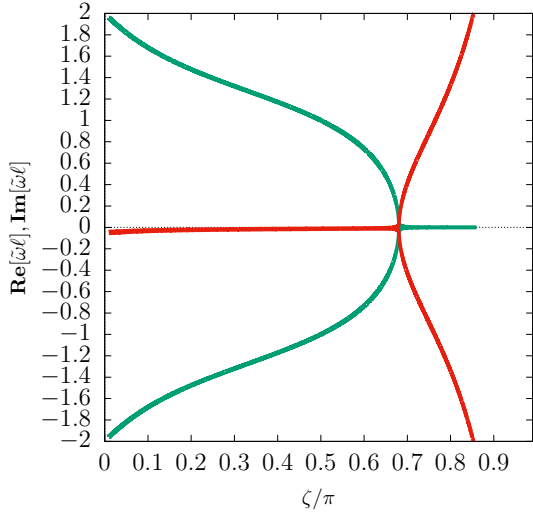


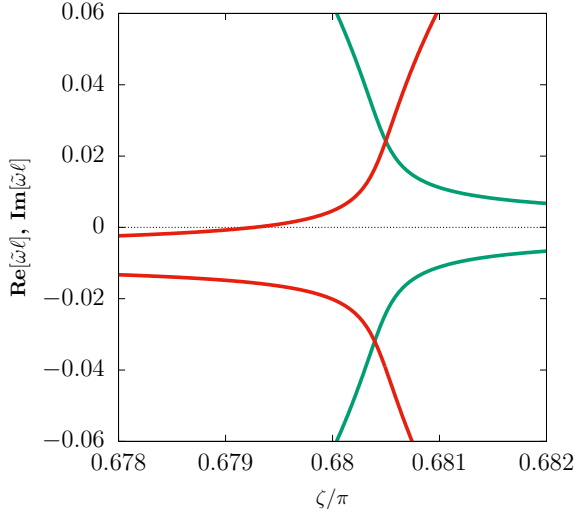
Figure 9. Same as Figures 1(a) and 1(b) but for the neutral field in the AdS black hole with $(r_+, r_-) = (0.1\ell, 0.001\ell)$.

2. Charged field

Figure 10(a) gives the relation between ζ and $\tilde{\omega}$ for the charged field with $eQ = 0.01$ in the AdS black hole with $(r_+, r_-) = (0.1\ell, 0.001\ell)$. Figure 10(b) is the enlarged figure of Figure 10(a) in the range of $\zeta/\pi \in [0.678, 0.682]$ and $\text{Im}[\tilde{\omega}\ell] \in [-0.06, 0.06]$. We note that the result for $eQ = -0.01$ gives the same graph. Figure 10(b) shows the existence of the boundary condition at the onset of instability $\zeta = \zeta_c$ such that $\text{Im}[\tilde{\omega}\ell] = 0$ but $\text{Re}[\tilde{\omega}\ell] \neq 0$. This mode is purely oscillative. This suggests a branch to nonlinearly oscillating solutions or charged oscillating black holes dubbed “black resonators” [3–5] in the AdS spacetime.



(a) The relation between ζ and $\tilde{\omega}$



(b) The enlarged figure of Figure 10(a).

Figure 10. Same as Figures 1(a) and 1(b) but for the charged field with $eQ = 0.01$ in the AdS black hole with $(r_+, r_-) = (0.1\ell, 0.001\ell)$.

3. Flow of QNFs with respect to ζ

Figures 11(a) and 11(b) show the flow of the QNFs in the complex plane for the neutral and charged fields, respectively, in the AdS black hole with $(r_+, r_-) = (0.1\ell, 0.001\ell)$. The green, red, and blue lines denote trajectories which the QNFs with $eQ = 0, -0.01, 0.01$ draw when we continuously change ζ . The arrows indicate the direction in which the QNF flows as ζ increases. In Figure 11(a), we can see that for the neutral field, the QNF for $\zeta < \zeta_b$ has a non-zero real part and a negative imaginary part. At $\zeta = \zeta_b$ slightly below ζ_0 , the QNF splits into two which have different imaginary parts but the same non-zero real part. The real part of these QNFs becomes zero at $\zeta = \zeta_0$. Then, the QNFs for $\zeta_0 < \zeta \leq \zeta_c$ are pure imaginary and both move along the arrow on the imaginary axis as ζ increases, the one goes up and the other down in the lower half plane. After that, the imaginary part of the QNF which is going up becomes zero at $\zeta = \zeta_c$, implying the onset of instability. We can see $\zeta_b < \zeta_0 < \zeta_c$. The flow described above is consistent with the symmetry $\omega \rightarrow -\omega^*$.

Figure 11(b) shows the flow for the charged field. The QNFs approach the imaginary axis as ζ increases. The one mode goes up and the other down along the axis as ζ increases. For $eQ > 0$, the QNF with $\text{Re}[\tilde{\omega}] > 0$ goes up, while that with $\text{Re}[\tilde{\omega}] < 0$ goes down. For $eQ < 0$, the result is opposite. This is a feature quite different from the neutral field. The

mode which goes up eventually causes superradiant instability at $\zeta = \zeta_c$. We can see that the flow is consistent with the symmetry $(\tilde{\omega}, eQ) \rightarrow (-\tilde{\omega}^*, -eQ)$.

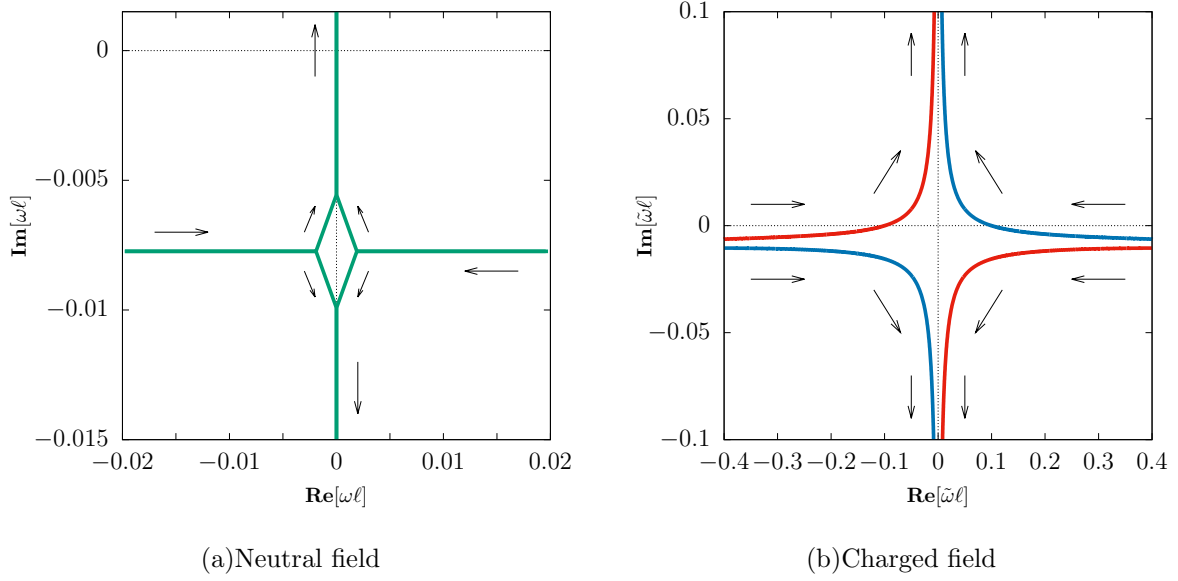


Figure 11. The flow of QNFs in the AdS black hole with $(r_+, r_-) = (0.1\ell, 0.001\ell)$. The $\tilde{\omega}$ moves as ζ is increased continuously. The green, red, and blue lines denote $eQ = 0, -0.01$, and 0.01 , respectively.

VI. PHYSICAL INTERPRETATION

A. Electromagnetic superradiance

From Eq. (2.10) and Eq. (4.5), we obtain the radial equation,

$$\left[-\frac{d^2}{dx^2} + V(x) \right] u(x) = \left(\tilde{\omega} - \frac{eQ}{r} \right)^2 u(x), \quad (6.1)$$

where

$$V(x) = \frac{\Delta}{r^2} \left[\frac{1}{r} \frac{d}{dr} \left(\frac{\Delta}{r^2} \right) + \frac{1}{r^2} \{ l(l+1) + \mu^2 r^2 \} \right]. \quad (6.2)$$

We assume $\omega \in \mathbb{R}$. The effective potential of the charged scalar field in the charged black hole can be negative near the outer horizon depending upon the charge of the field. The region, where the effective potential is negative, is called the generalised ergoregion [28].

Here, we first discuss electromagnetic superradiance for a massless charged scalar field in the charged black hole spacetime with $\mu^2 = \Lambda = 0$, which gives an important background

for the physical interpretation of the electromagnetic superradiance in the AdS system. In the limit of $x \rightarrow \infty$, Eq. (6.1) is reduced to

$$\left[\frac{d^2}{dx^2} + \tilde{\omega}^2 \right] u(x) \simeq 0, \quad (6.3)$$

and we obtain the general solution of Eq. (6.3) as

$$u(x) \sim A_{\text{in}} e^{-i\tilde{\omega}x} + A_{\text{out}} e^{i\tilde{\omega}x}, \quad A_{\text{in}}, A_{\text{out}} \in \mathbb{C}. \quad (6.4)$$

The subscripts "in" and "out" denote the ingoing and outgoing modes at the conformal infinity, respectively.

Noting the conservation of the number current given by Eq. (2.11), we find

$$\tilde{\omega}(|A_{\text{in}}|^2 - |A_{\text{out}}|^2) = \left(\tilde{\omega} - \frac{eQ}{r_+} \right) |B_{\text{in}}|^2 r_+^2, \quad (6.5)$$

where we have used the asymptotic solutions (4.9) with $B_{\text{out}} = 0$ and Eq. (6.4). Thus, we can observe that the amplitude of the reflected wave is larger than that of the incident wave, i.e.

$$|A_{\text{out}}|^2 > |A_{\text{in}}|^2, \quad (6.6)$$

if the mode with $eQ > 0$ satisfies

$$0 < \tilde{\omega} < \frac{eQ}{r_+}, \quad (6.7)$$

or if the mode with $eQ < 0$ satisfies

$$\frac{eQ}{r_+} < \tilde{\omega} < 0. \quad (6.8)$$

This amplification of the wave is called electromagnetic superradiance.

Using Eq. (6.4), the conservation of j^a and $j_{(e)}^a$ are integrated to give

$$j^r(t, r, \theta, \phi) = 2\tilde{\omega}(|A_{\text{out}}|^2 - |A_{\text{in}}|^2) \frac{|Y_{lm}(\theta, \phi)|^2}{r^2}, \quad (6.9)$$

and

$$j_{(e)}^r(t, r, \theta, \phi) = 2e\tilde{\omega}(|A_{\text{out}}|^2 - |A_{\text{in}}|^2) \frac{|Y_{lm}(\theta, \phi)|^2}{r^2}, \quad (6.10)$$

respectively, for $r_+ \leq r < \infty$. Therefore, there are a net positive (negative) outgoing number current and therefore net positive (negative) outgoing electric current for $\tilde{\omega} > (<)0$. We can conclude that a net positive (negative) particle number and net positive (negative) charge

are extracted from the system for $\tilde{\omega} > (< 0)$ and they must be extracted from the black hole. We will see that this is really the case in Section VIC.

Here we see the energetics of the system. The outgoing energy current of the scalar field in the asymptotic region can be calculated to

$$J_{(m)}^r \simeq 2\tilde{\omega}^2(|A_{\text{out}}|^2 - |A_{\text{in}}|^2) \frac{|Y_{lm}(\theta, \phi)|^2}{r^2} \quad \text{as } r \rightarrow \infty, \quad (6.11)$$

while the energy current by the electromagnetic field vanishes there. Therefore, positive energy is extracted from the system in the superradiance. However, it does not necessarily mean that this positive energy must be extracted from the black hole because $J_{(m)}^a$ is not a conserved current as $\nabla_a J_{(m)}^a = -\nabla_a J_{(em)}^a$. In general, since $\nabla^a T_{(em)ab} = j_{(e)}^a F_{ab}$, we obtain $\nabla_a J_{(em)}^a = -j_{(e)}^a \xi^b F_{ab}$. In the present system, this implies

$$\nabla_a J_{(em)}^a = -j_{(e)}^r F_{rt}. \quad (6.12)$$

This shows that the electromagnetic field loses energy due to the work on the electric current exerted by the electric field. On the other hand, this implies

$$\nabla_a J_{(m)}^a = j_{(e)}^r F_{rt} \quad (6.13)$$

Thus, the scalar field receives energy through the work on the electric current exerted by the electric field. We can easily integrate Eq. (6.13) putting Eq. (6.10) in the source term and fix the function of integration using Eq. (6.11). Thus, we obtain

$$J_{(m)}^r = 2\tilde{\omega} \left(\tilde{\omega} - \frac{eQ}{r} \right) (|A_{\text{out}}|^2 - |A_{\text{in}}|^2) \frac{|Y_{lm}|^2}{r^2} \quad (6.14)$$

for $r_+ \leq r < \infty$. We can see that under the condition for the superradiance, $J_{(m)}^r$ is necessarily negative at $r = r_+$. Therefore, there is a net ingoing energy current at the horizon. $J_{(m)}^r$ changes its sign at $r = r_S = eQ/\tilde{\omega}$. There is a net ingoing energy current for $r_+ \leq r < r_S$, while a net outgoing energy current for $r > r_S$. The radius r_S thus characterises the energy injection from the electric field into the scalar field. The superradiance in the present system extracts energy not from the black hole but from its ambient electric field. In Section VIC, we will explicitly see that the superradiance extracts not energy but charge from the black hole.

In the AdS charged black hole, we can show that all of $\sqrt{-g}j^r$, $\sqrt{-g}j_{(e)}^r$, and $\sqrt{-g}J^r$ vanish at the conformal infinity by using the asymptotic behaviour (4.22) under the Robin

boundary condition (3.16). Therefore, the outgoing and ingoing waves must cancel out each other there. This means that the Robin boundary condition makes the conformal boundary perfectly reflective. Since we can regard the overlapping region between the near and far regions as the asymptotically flat region both from the black hole and from the conformal infinity, we can interpret the superradiance instability in the present system as follows. The ingoing wave in the overlapping region is reflected and amplified by electromagnetic superradiance near the black hole. This amplified outgoing wave goes through the overlapping region and perfectly reflected by the AdS boundary under the Robin boundary. This reflected ingoing wave goes through the asymptotic region and becomes the incident wave to the black hole again. A series of these successive processes results in the superradiance instability. The scalar field takes charge from the black hole and energy from its ambient electric field and gives energy to the black hole. The black hole takes energy from and gives charge to the scalar field.

B. Particle picture

We would like to interpret the electromagnetic superradiance in terms of the particle picture. Since the electric charge density and particle number density measured by the Killing observer with the 4-velocity $u^a = \xi^a / \sqrt{-\xi^a \xi_a}$ are given by

$$-u^a j_a = \frac{2\tilde{\omega}|\Psi|^2}{\sqrt{-g_{tt}}} \quad \text{and} \quad -u^a (j_{(e)})_a = \frac{2e\tilde{\omega}|\Psi|^2}{\sqrt{-g_{tt}}}, \quad (6.15)$$

respectively, the number density is positive (negative) and the electric charge density is positive (negative) if $\tilde{\omega} > (<)0$. Therefore, the positive-frequency and negative-frequency modes are regarded as associated with a particle with charge $+e$ and anti-particle with charge $-e$, respectively.

The conserved energy for a particle with charge q is given by

$$E = -(\partial_t)^a p_a = -\pi_t - qA_t = -\pi_t + \frac{qQ}{r} + q\phi_0, \quad (6.16)$$

where $p^a = \pi^a + qA^a$, and q and π^a are the charge and the 4-momentum of the charged particle measured by a local observer, respectively. For a massive particle of mass m , $\pi^a = mu^a$, while for a massless particle, $\pi^a = k^a$. We can identify the redefined conserved energy $E - q\phi_0$ with $\tilde{\omega}$ because $\tilde{\omega}$ is constant over the mode and is associated with the Killing time

t at the infinity. Eq. (6.16) can then be rewritten in the form

$$\omega_K = \tilde{\omega} - \frac{qQ}{r}, \quad (6.17)$$

where $\omega_K := -\pi_t$ is the frequency of the particle measured by the local Killing observer in terms of the Killing time t .

Let us put $q = e$ as suggested by the relation between the electric current density and particle number current density. For $eQ > 0$, ω_K is negative in the vicinity of the horizon if

$$0 < \tilde{\omega} < \frac{eQ}{r_+}. \quad (6.18)$$

Therefore, the superradiance condition (6.7) is equivalent to that for the existence of the *locally negative-energy state* ($\omega_K < 0$) in the vicinity of the horizon for the *positive-energy particle* ($\tilde{\omega} > 0$) at the infinity.

Then, what does the superradiance condition (6.8) for $eQ < 0$ mean? Applying the above discussion to the present case, the condition (6.8)

$$\frac{eQ}{r_+} < \tilde{\omega} < 0 \quad (6.19)$$

is interpreted as the existence of the *locally positive-energy state* ($\omega_K > 0$) in the vicinity of the horizon for the *negative-energy antiparticle* ($\tilde{\omega} < 0$) at the infinity.

Therefore, the occurrence of the superradiance for $eQ > 0$ decreases the total charge of the system, while increases for $eQ < 0$. This is consistent with a view that the particles or antiparticles carry the charge of the same sign as that of the black hole away from the system. We can conclude that the superradiance of the complex scalar field in the Reissner-Nordström black hole is a counterpart of discharging a black hole by the Schwinger effect in quantum field theory.

In the above, we have implicitly assumed that the spacetime is asymptotically flat. In the small AdS black hole, we can expect that the above particle picture is still valid, where the overlapping region between the near and far regions is regarded as the asymptotically flat region from the black hole. On the other hand, if we consider the perfectly reflective boundary condition at the conformal infinity, the outgoing particles and antiparticles are bounced back and confined within the system. Thus, after some span of evolution, the total number and charge of the particles or antiparticles confined within the system will become so significant that the test particle approximation will no longer be valid and the backreaction of these particles must be seriously considered.

C. Thermodynamical insight

Here we discuss a thermodynamical argument. We explicitly calculate the energy current and electric current ingoing into the horizon, $J_a n^a|_{\mathcal{H}_+}$ and $j_{(e)a} n^a|_{\mathcal{H}_+}$, respectively, where $n^a = -\xi^a$ at the outer horizon for the static black hole. To avoid the coordinate singularity at the outer horizon, we use the ingoing Eddington-Finkelstein coordinates

$$ds^2 = -\frac{\Delta}{r^2} dv^2 + 2dvdr + r^2(d\theta^2 + \sin^2\theta d\phi^2), \quad (6.20)$$

where $v = t + x + \text{const}$ and the gauge field takes the form

$$A_\mu dx^\mu = -\left(\frac{Q}{r} + \phi_0\right) dv + \frac{r^2}{\Delta} \left(\frac{Q}{r} + \phi_0\right) dr. \quad (6.21)$$

Near the outer horizon, the scalar field satisfying the ingoing-wave condition behaves as

$$\Psi \sim e^{-i\omega v + i\left(\frac{eQ}{r_+} + e\phi_0\right)x} Y_{lm}(\theta, \phi). \quad (6.22)$$

Assuming that $\tilde{\omega} = \tilde{\omega}_R + i\tilde{\omega}_I$ is complex, we obtain the following result:

$$J_{(m)a} n^a|_{\mathcal{H}_+} = 2 \left| \tilde{\omega} - \frac{eQ}{r_+} \right|^2 |\Psi|^2, \quad (6.23)$$

$$J_{(em)a} n^a|_{\mathcal{H}_+} = 0, \quad (6.24)$$

$$j_{(e)a} n^a|_{\mathcal{H}_+} = 2e \left(\tilde{\omega}_R - \frac{eQ}{r_+} \right) |\Psi|^2. \quad (6.25)$$

Eq. (6.23) implies that no energy can be extracted from the black hole irrespective of the value of $\tilde{\omega}$.

Assuming a quasistatic change, we can also find

$$\Delta Q = \frac{e \left(\tilde{\omega}_R - \frac{eQ}{r_+} \right)}{\left| \tilde{\omega} - \frac{eQ}{r_+} \right|^2} \Delta M \quad (6.26)$$

with $\Delta M \geq 0$.

We can see that if the superradiance condition is satisfied in terms of $\tilde{\omega}_R$, we can conclude that $\Delta|Q| < 0$, that is, the black hole is discharged by the scalar field. This is because if $eQ > 0$, Eqs. (6.7) and (6.25) imply $e\Delta Q < 0$, whereas if $eQ < 0$, Eqs. (6.8) and (6.25) imply $e\Delta Q > 0$.

Next we see the change in the area of the black hole due to the superradiance. In the near region, the metric can be well approximated by the Reissner-Nordström metric for the

black hole much smaller than the AdS length. Since the area of the Reissner-Nordström black hole is given by $A = 4\pi r_+^2$, its increase in a quasistatic process is calculated to

$$\Delta A = 8\pi r_+ \frac{r_+ \Delta M - Q \Delta Q}{\sqrt{M^2 - Q^2}}. \quad (6.27)$$

As is well known, this can be recast to the following more familiar form:

$$\Delta M = \frac{\kappa}{8\pi} \Delta A + \Phi_H \Delta Q, \quad (6.28)$$

where the surface gravity κ and the surface electric potential Φ_H are given by

$$\kappa = \frac{\sqrt{M^2 - Q^2}}{r_+^2} \quad \text{and} \quad \Phi_H = \frac{Q}{r_+}, \quad (6.29)$$

respectively. This implies

$$\Delta A = \frac{8\pi}{\kappa} \frac{\left(\tilde{\omega}_R - \frac{eQ}{r_+}\right) \left(\tilde{\omega}_R - \frac{2eQ}{r_+}\right) + \tilde{\omega}_I^2}{\left|\tilde{\omega} - \frac{eQ}{r_+}\right|^2} \Delta M. \quad (6.30)$$

Since the null energy condition is satisfied in the present system and the boundary condition at the conformal infinity uniquely determines the time development of the scalar field, we can expect that the area law of the AdS black hole holds in an appropriate formulation [34]. We can see that the superradiance conditions given by Eqs. (6.7) and (6.8) in terms of $\tilde{\omega}_R$ imply $\Delta A \geq 0$ for $eQ > 0$ and $eQ < 0$, respectively. Therefore, from a thermodynamical point of view, we conclude that the black hole may remain the (approximate) Reissner-Nordström solution with increasing its mass, decreasing the absolute value of its charge, and therefore increasing its area in a quasistatic manner during the superradiance instability, as long as the black hole is much smaller than the AdS length.

VII. CONCLUSION

In this paper, we have extended the result of [1] for a neutral massive scalar field in the AdS spacetime to charged and neutral massive scalar fields in a charged AdS black hole. In Section IV, we have clarified the parameter range for which the matched asymptotic expansion method applies for charged massive scalar fields and derived an equation which determines QNFs. In Section V, we have discussed the relation between the parameter of the boundary condition at the conformal infinity, $\zeta \in [0, \pi]$, and the QNFs of the scalar field in the AdS black holes with $(r_+, r_-) = (0.01\ell, 0.001\ell)$ and $(r_+, r_-) = (0.1\ell, 0.001\ell)$.

We have shown that the first fundamental mode of the neutral scalar field in the AdS black hole has a critical value ζ_0 beyond which the real part of the QNF becomes zero. We note that such a critical value does not exist for the second fundamental mode. We have also shown that there exist another two critical values, ζ_b and ζ_c , corresponding to the bifurcation and the onset of instability, respectively. Furthermore, we find $\zeta_b < \zeta_0 < \zeta_c$. For $\zeta_c < \zeta$, there are two QNFs that have zero real part but positive and negative values for the imaginary part. This result indicates instability for $\zeta_c < \zeta$. From the fact that the equation of motion for the neutral field ψ can be written in the form of $A\psi = \omega^2\psi$, where A and ω denote, respectively, the linear operator and the frequency of the mode, we can see that A fails to be positive for $\zeta_c < \zeta$, where ω is pure imaginary. Since the field is neutral, there is no superradiance. Hence, this instability arises from the boundary condition. The time scale of the instability becomes shorter as ζ increases. At $\zeta = \zeta_c$, there exists a static neutral perturbation in the charged AdS black hole. For $\zeta < \zeta_c$, the evolution is stable and the time scale of the decay becomes longer as ζ increases. Moreover, we analytically and numerically establish that although the system of the neutral field in the AdS spacetime has both symmetries $\omega \rightarrow -\omega$ and $\omega \rightarrow \omega^*$, the existence of the black hole horizon breaks them. Instead, a symmetry $\omega \rightarrow -\omega^*$ remains for the neutral field on the AdS black hole spacetime.

The charged scalar field has no critical value at which the real part of the QNF becomes zero. The results we have shown imply that the evolution of the charged field can be unstable by electromagnetic superradiance whether the charge is negative or positive. Actually, for any ζ we investigated, all of the unstable modes satisfy the superradiant condition, while none of the stable modes does. The instability can be caused by the charged scalar field even for $\zeta \leq \zeta_0$, where ζ_0 is the critical value at which $\text{Re}[\omega] = 0$ for *the neutral field*. This is remarkably different from for the neutral field. Furthermore, the evolution is unstable for $\zeta_c < \zeta$. The time scale of the instability for $\zeta_0 < \zeta$ can be much shorter than that for $\zeta \leq \zeta_0$. In this sense, the superradiant instability can be enhanced by the boundary condition. On the other hand, the modes that do not satisfy the superradiant condition are stable for $\zeta \leq \zeta_0$. We point out that the symmetry $\tilde{\omega} \rightarrow -\tilde{\omega}^*$, which exists for the neutral field, is broken. Actually, the symmetry is deformed to $(\tilde{\omega}, eQ) \rightarrow (-\tilde{\omega}^*, -eQ)$. We show that the superradiance in this system extracts energy not from the black hole but from its ambient electric field and that it extract charge from the black hole and thus weaken its

ambient electric field. The Robin boundary condition makes the conformal infinity perfectly reflective, so that the superradiance induces instability. This can be interpreted as a classical scalar-field counterpart of discharging a black hole by the Schwinger effect. The black hole increases its mass, decreases the absolute value of its charge, and increases its area, as long as the black hole is much smaller than the AdS length.

The numerical result in this paper is restricted to black holes much smaller than the AdS length scale. It suggests that the radius of the black hole may increase in a quasistatic manner and that it can go beyond the regime of small black holes. On the other hand, the instability of large charged AdS black holes has been intensively discussed in terms of the holographic superconductor. In the context of AdS/CFT correspondence, the instabilities of the AdS black hole are expected to imply the phase transition of dual theories. Our result suggests the new dynamics of the dual quantum field theory. Also, we would like to know the final fate of the instabilities. Recently, Ref. [6] has shown the existence of static solitons in the 4-dimensional AdS spacetime with the boundary condition corresponding to $\zeta_c < \zeta$. Their result suggests the existence of black hole solutions with a non-trivial scalar field satisfying the boundary condition $\zeta_c < \zeta$. Then, the hairy black hole solution could be a candidate for the final fate of the instabilities we have shown. These problems remain for our outlook.

ACKNOWLEDGMENTS

The authors are grateful to Akihiro Ishibashi for his helpful comments. The authors would like to thank Masashi Kimura, Keiju Murata, and Takaaki Ishii for the informative comments. TK acknowledges Shunichiro Kinoshita and Shin Nakamura for the hospitality and the helpful comments on the seminar at particle theory group in Chuo university. The authors also thank the workshop “GR in AdS”. This work was supported by Rikkyo University Special Fund for Research (TK) and JSPS KAKENHI Grant Numbers JP19K03876 (TH).

Appendix A: Positive self-adjoint extension of symmetric operators

Here we provide definitions for the mathematical notions used in Section III.

A subset D of \mathcal{H} is said to be *dense* if D satisfies $\mathcal{H} = \bar{D}$, where \bar{D} is the closure of D . A vector $\psi \in \mathcal{H}$ is said to be *normalisable* if and only if $(\psi, \psi) < \infty$. The domain of a linear operator \mathcal{O} is denoted by $D(\mathcal{O})$.

A linear operator \mathcal{O} is said to be *positive* if and only if $(\psi, \mathcal{O}\psi) > 0$ for any nonzero vector $\psi \in D(\mathcal{O})$, where (\cdot, \cdot) stands for the inner product. A linear operator \mathcal{P} is said to be an *adjoint* of \mathcal{O} if and only if $(\psi, \mathcal{O}\phi) = (\mathcal{P}\psi, \phi)$ and $\mathcal{P}\psi = \Theta$ for any vectors $\phi \in D(\mathcal{O})$, $\psi \in D(\mathcal{P})$ and $\Theta \in \mathcal{H}$. The adjoint of \mathcal{O} is denoted by \mathcal{O}^* . A linear operator \mathcal{P} is said to be an *extension* of \mathcal{O} if and only if $D(\mathcal{O}) \subset D(\mathcal{P})$.

A linear operator \mathcal{O} is said to be *symmetric* if all of the following three conditions are satisfied: (i) $D(\mathcal{O})$ is dense, (ii) $(\psi, \mathcal{O}\phi) = (\mathcal{O}\psi, \phi)$ for any vectors $\psi, \phi \in D(\mathcal{O})$, and (iii) $D(\mathcal{O}) \subset D(\mathcal{O}^*)$. Therefore, the adjoint of a symmetric operator is an extension of the symmetric operator.

A symmetric operator \mathcal{O} is said to be *bounded below* if and only if there exists $\gamma \in \mathbb{R}$ such that $(\mathcal{O}\psi, \psi) \geq \gamma(\psi, \psi)$ for any vector $\psi \in D(\mathcal{O})$. A symmetric operator is said to be *unbounded below* if and only if it is not bounded below.

A linear operator \mathcal{O} is said to be *self-adjoint* if and only if all of the following three conditions are satisfied: (i) $D(\mathcal{O})$ is dense, (ii) $(\psi, \mathcal{O}\phi) = (\mathcal{O}\psi, \phi)$ for any vectors $\psi, \phi \in D(\mathcal{O})$, and (iii) $D(\mathcal{O}) = D(\mathcal{O}^*)$. One can obtain a self-adjoint operator by extending a symmetric operator [25, 32]. Thus obtained self-adjoint operator is called *self-adjoint extension*.

Appendix B: Validity of the matching of the near-region and far-region solutions

We introduce a small parameter $\epsilon = r_+/\ell$ and a nondimensional coordinate $x = r/r_+$. First we focus on the validity of the near-horizon solution. Eq. (4.15) is rewritten in the form

$$\begin{aligned} \mathcal{E}_1(x) = & -\frac{(\epsilon x)^2}{1 - \frac{r_-}{r_+}} \left[-\mu^2 \ell^2 \left(x - \frac{r_-}{r_+} \right) + (\tilde{\omega} \ell)^2 (1+x) \left(1 + \frac{1}{x^2} \right) \right. \\ & \left. - 2(\tilde{\omega} \ell) \left(\frac{eQ}{\epsilon} \right) \left(1 + \frac{1}{x} + \frac{1}{x^2} \right) + \left(\frac{eQ}{\epsilon} \right)^2 \left(\frac{1}{x} + \frac{1}{x^2} \right) \right]. \end{aligned} \quad (\text{B1})$$

Because $-(\tilde{\omega}\ell)(eQ) \leq |\tilde{\omega}\ell||eQ|$, we find an inequality $|\mathcal{E}_1(x)| \leq \tilde{\mathcal{E}}_1(x)$, where we have defined

$$\begin{aligned} \tilde{\mathcal{E}}_1(x) := & \frac{(\epsilon x)^2}{1 - \frac{r_-}{r_+}} \left[-\mu^2 \ell^2 \left(x - \frac{r_-}{r_+} \right) + |\tilde{\omega}\ell|^2 (1+x) \left(1 + \frac{1}{x^2} \right) \right. \\ & \left. + 2|\tilde{\omega}\ell| \left(\frac{|eQ|}{\epsilon} \right) \left(1 + \frac{1}{x} + \frac{1}{x^2} \right) + \left(\frac{|eQ|}{\epsilon} \right)^2 \left(\frac{1}{x} + \frac{1}{x^2} \right) \right]. \end{aligned} \quad (\text{B2})$$

Here we note that $\tilde{\mathcal{E}}_1(x)$ is an increasing function of x . In the limit of $1 \ll x$, the asymptotic behaviour of $\tilde{\mathcal{E}}_1(x)$ can be written as

$$\tilde{\mathcal{E}}_1(x) \simeq x \left[\{|\tilde{\omega}\ell|(\epsilon x) + |eQ|\}^2 - \mu^2 \ell^2 (\epsilon x)^2 \right]. \quad (\text{B3})$$

As for $|ab|$, we have an inequality

$$1 < |ab| = \sqrt{4\sigma^2 + (l+1)^2}. \quad (\text{B4})$$

Hence, $|\mathcal{E}_1(x)| \ll |ab|$ is satisfied in the region given by $1 < x \leq x_0$, if x_0 satisfies $1 \ll x_0 \ll 1/\epsilon$ and

$$\tilde{\mathcal{E}}_1(x_0) \ll 1 \Leftrightarrow \epsilon^2 \left\{ \left(|\tilde{\omega}\ell| + \frac{|eQ|}{\epsilon} \frac{1}{x_0} \right)^2 - \mu^2 \ell^2 \right\} \ll \frac{1}{x_0^3}. \quad (\text{B5})$$

Assuming $\tilde{\omega}\ell = O(1)$ and $eQ = o(\epsilon^{1/3+\delta})$, we find that if we take $x_0 = c_0 \epsilon^{-2/3+\delta}$ with $c_0 = O(1)$ and $0 < \delta < 2/3$, the inequality (B5) is satisfied.

Next we focus on the validity of the far-region solution. Clearly, Eq. (4.20) is reduced to Eq. (3.11) for the neutral scalar field because of $\mathcal{E}_2(r) = 0$. For the charged field, we can approximate Eq. (4.20) to Eq. (3.11) if $\mathcal{E}_2(r)$ satisfies $h(y)|\mathcal{E}_2(y)| \ll 1$, where we have defined

$$h(y) := \frac{|g(y)|}{|y(1-y)\frac{d^2}{dy^2}g(y)| + |\{\gamma - (\alpha + \beta + 1)y\}\frac{d}{dy}g(y)| + |-\alpha\beta g(y)|}. \quad (\text{B6})$$

Substituting Eq. (3.13) into the above $g(y)$, we notice $\max h(y) = \mathcal{O}(1)$ for $y \lesssim 200$ with $|\tilde{\omega}\ell| = \mathcal{O}(1)$, $l = \mathcal{O}(1)$. Hence, the charged scalar field in the far region can be described by the Gaussian hypergeometric functions if $|\mathcal{E}_2(y)| \ll 1$ is satisfied. We shall discuss whether $|\mathcal{E}_2(y)| \ll 1$ is satisfied. In terms of ϵ and x , $\mathcal{E}_2(y)$ is rewritten as

$$\mathcal{E}_2(x) = \frac{1}{4(\epsilon x)^2} \frac{1}{1 + (\epsilon x)^2} \left\{ 2(\tilde{\omega}\ell)(eQ)(\epsilon x) - (eQ)^2 \right\}. \quad (\text{B7})$$

Noting $-(\tilde{\omega}\ell)(eQ) \leq |\tilde{\omega}\ell||eQ|$, we find

$$|\mathcal{E}_2(x)| \leq \tilde{\mathcal{E}}_2(x), \quad (\text{B8})$$

where we have defined

$$\tilde{\mathcal{E}}_2(x) := \frac{1}{4(\epsilon x)^2} \frac{1}{1 + (\epsilon x)^2} \{2|\tilde{\omega}\ell||eQ|(\epsilon x) + |eQ|^2\}. \quad (\text{B9})$$

Note that $\tilde{\mathcal{E}}_2(x)$ is a decreasing function of x and $\tilde{\mathcal{E}}_2(x) \ll 1$ in the limit of $x \rightarrow \infty$. Therefore, if we can find x_1 such that $\tilde{\mathcal{E}}_2(x_1) \ll 1$ and $1 \ll x_1 \ll 1/\epsilon$, $|\mathcal{E}_2(x)| \ll 1$ is satisfied for $x_1 \leq x$. Assuming $|eQ| \ll \epsilon x_1$ and $\tilde{\omega}\ell = O(1)$, $|\mathcal{E}_2(y)| \ll 1$ holds for $x_1 \leq x < \infty$.

Finally, we discuss whether there is an overlapping region, where both the near-region and far-region solutions are valid. For the neutral field, we can match them without further discussion. The reason is that the far-region approximate solution (3.17) can describe the field everywhere in the region $1 \ll x$ and the near-region approximate solution (4.18) is valid in $1 \ll x \leq x_0$ such that $1 \ll x_0 \ll 1/\epsilon$ because there exists x_0 such that the inequality (B5) is satisfied for $eQ = 0$ under the assumption $|\omega\ell| = \mathcal{O}(1)$. For the charged field case, assuming $|eQ| = o(\epsilon^{1/3+\delta})$ and $|\tilde{\omega}\ell| = O(1)$, if we choose $x_0 = c_0\epsilon^{-2/3+\delta}$ and $x_1 = c_1\epsilon^{-2/3+\delta}$ with $0 < c_1 < c_0$ and $0 < \delta < 2/3$, both $\tilde{\mathcal{E}}_1 \ll 1$ and $\tilde{\mathcal{E}}_2 \ll 1$ are satisfied for $x_1 \leq x \leq x_0$. Therefore, we can identify the overlapping region with the interval $x_1 \leq x \leq x_0$.

Appendix C: Asymptotic behaviours of the near-region and far-region solutions

We are interested in the asymptotic behaviour of the far-region solution (3.17) at $y \simeq 1$. Using the transformation formula of the Gaussian hypergeometric functions [27], we obtain

$$\begin{aligned} F\left(\alpha, \alpha - \gamma + 1; \alpha - \beta + 1; \frac{1}{y}\right) &= y^{\alpha-\gamma+1} (y-1)^{\gamma-\alpha-\beta} \frac{\Gamma(\alpha-\beta+1)\Gamma(\alpha+\beta-\gamma)}{\Gamma(\alpha)\Gamma(\alpha-\gamma+1)} \\ &\quad \times F(1-\alpha, 1-\beta; \gamma-\alpha-\beta; y-1) \\ &\quad + y^\alpha \frac{\Gamma(\alpha-\beta+1)\Gamma(\gamma-\alpha-\beta)}{\Gamma(1-\beta)\Gamma(\gamma-\beta)} \\ &\quad \times F(\alpha, \beta; \alpha+\beta-\gamma+1; y-1), \end{aligned} \quad (\text{C1})$$

and

$$\begin{aligned}
F\left(\beta, \beta - \gamma + 1; \beta - \alpha + 1; \frac{1}{y}\right) &= y^{\beta - \gamma + 1} (y - 1)^{\gamma - \alpha - \beta} \frac{\Gamma(\beta - \alpha + 1) \Gamma(\alpha + \beta - \gamma)}{\Gamma(\beta) \Gamma(\beta - \gamma + 1)} \\
&\times F(1 - \alpha, 1 - \beta; \gamma - \alpha - \beta; y - 1) \\
&+ y^\beta \frac{\Gamma(\beta - \alpha + 1) \Gamma(\gamma - \alpha - \beta)}{\Gamma(1 - \alpha) \Gamma(\gamma - \alpha)} \\
&\times F(\alpha, \beta; \alpha + \beta - \gamma + 1; y - 1).
\end{aligned} \tag{C2}$$

Therefore Eq. (3.17) is rewritten in the form

$$\begin{aligned}
\psi(y) &= D y^{\frac{\tilde{\omega}\ell}{2}} (y - 1)^{\frac{l}{2}} \\
&\times \left[y^{-\gamma + 1} (y - 1)^{\gamma - \alpha - \beta} \Gamma(\alpha + \beta - \gamma) \left(\frac{\kappa \Gamma(\alpha - \beta + 1)}{\Gamma(\alpha) \Gamma(\alpha - \gamma + 1)} + \frac{\Gamma(\beta - \alpha + 1)}{\Gamma(\beta) \Gamma(\beta - \gamma + 1)} \right) \right. \\
&\times F(1 - \alpha, 1 - \beta; \gamma - \alpha - \beta; y - 1) \\
&+ \Gamma(\gamma - \alpha - \beta) \left(\frac{\kappa \Gamma(\alpha - \beta + 1)}{\Gamma(1 - \beta) \Gamma(\gamma - \beta)} + \frac{\Gamma(\beta - \alpha + 1)}{\Gamma(1 - \alpha) \Gamma(\gamma - \alpha)} \right) \\
&\left. \times F(\alpha, \beta; \alpha + \beta - \gamma + 1; y - 1) \right].
\end{aligned} \tag{C3}$$

The above expression gives the asymptotic behaviour (3.18).

Next we are interested in the asymptotic behaviour of the near-region solution (4.18) at $z \simeq 1$. Using the transformation formula of the Gaussian hypergeometric functions [27],

$$\begin{aligned}
F(1 - c + a, 1 - c + b; 2 - c; z) &= \frac{\Gamma(2 - c) \Gamma(c - a - b)}{\Gamma(1 - a) \Gamma(1 - b)} \\
&\times F(1 - c + a, 1 - c + b; -c + a + b + 1; 1 - z) \\
&+ (1 - z)^{c - a - b} \frac{\Gamma(2 - c) \Gamma(-c + a + b)}{\Gamma(1 - c + a) \Gamma(1 - c + b)} \\
&\times F(1 - a, 1 - b; c - a - b + 1; 1 - z).
\end{aligned} \tag{C4}$$

Therefore, the near-region solution (4.18) is rewritten in the form

$$\begin{aligned}
\psi(z) &= B z^{-i\sigma} \Gamma(1 - 2i\sigma) \left[\frac{\Gamma(-2l - 1)}{\Gamma(-2i\sigma - l) \Gamma(-l)} (1 - z)^{l+1} \right. \\
&\times F(1 - c + a, 1 - c + b; -c + a + b + 1; 1 - z) \\
&+ \frac{\Gamma(2l + 1)}{\Gamma(-2i\sigma + l + 1) \Gamma(l + 1)} (1 - z)^{-l} \\
&\left. \times F(1 - a, 1 - b; c - a - b + 1; 1 - z) \right].
\end{aligned} \tag{C5}$$

From the above expression, we obtain the asymptotic form (4.23) with Eq. (4.24).

Appendix D: Symmetry $(\omega, eQ) \rightarrow (-\omega^*, -eQ)$ in the matched asymptotic expansion

Note that σ is transformed to $-\sigma^*$ by this transformation. Then, the left-hand side of Eq. (4.25) is transformed as

$$\frac{B_1(\tilde{\omega}, \sigma)}{B_2(\tilde{\omega}, \sigma)} \rightarrow \frac{B_1(-\tilde{\omega}^*, -\sigma^*)}{B_2(-\tilde{\omega}^*, -\sigma^*)} = \left(\frac{B_1(\tilde{\omega}, \sigma)}{B_2(\tilde{\omega}, \sigma)} \right)^*, \quad (\text{D1})$$

because $B_1(\tilde{\omega}, \sigma)$ and $B_2(\tilde{\omega}, \sigma)$ satisfy the relation $B_1(\tilde{\omega}, \sigma) = B_1^*(-\tilde{\omega}^*, -\sigma^*)$ and $B_2(\tilde{\omega}, \sigma) = B_2^*(-\tilde{\omega}^*, -\sigma^*)$. Next, the right-hand side of Eq. (4.25) is transformed as

$$\frac{D_1(\tilde{\omega}, \kappa)}{D_2(\tilde{\omega}, \kappa)} \rightarrow \frac{D_1(-\tilde{\omega}^*, \kappa)}{D_2(-\tilde{\omega}^*, \kappa)} = \left(\frac{D_1(\tilde{\omega}, \kappa)}{D_2(\tilde{\omega}, \kappa)} \right)^*, \quad (\text{D2})$$

because of $D_1(\tilde{\omega}, \kappa) = D_1^*(-\tilde{\omega}^*, \kappa)$ and $D_2(\tilde{\omega}, \kappa) = D_2^*(-\tilde{\omega}^*, \kappa)$ as stated below Eq. (3.20). Hence, this transformation brings Eq. (4.25) to

$$\left(\frac{B_1(\tilde{\omega}, \sigma)}{B_2(\tilde{\omega}, \sigma)} \right)^* = \ell^{2l+1} \left(\frac{D_1(\tilde{\omega}, \kappa)}{D_2(\tilde{\omega}, \kappa)} \right)^*. \quad (\text{D3})$$

Since the above is nothing but the complex conjugate of Eq. (4.25), the solution of the above is the same as the solution obtained before the transformation. Thus, the symmetry for the charged scalar field in the charged black hole is given by $(\tilde{\omega}, eQ) \rightarrow (-\tilde{\omega}^*, -eQ)$.

-
- [1] A. Ishibashi and R. M. Wald, *Class. Quant. Grav.* **21**, 2981 (2004)
 - [2] R.M. Wald, *J. Math. Phys.* **21**, 2802 (1980).
 - [3] O. J. C. Dias, J. E. Santos and B. Way, *JHEP* **1512**, 171 (2015)
 - [4] T. Ishii and K. Murata, *Class. Quant. Grav.* **36**, no. 12, 125011 (2019)
 - [5] T. Ishii and K. Murata, *Class. Quant. Grav.* **37**, no. 7, 075009 (2020)
 - [6] P. Bizon, D. Hunik-Kostyra and M. Maliborski, arXiv:2001.03980 [gr-qc].
 - [7] J. M. Maldacena, *Int. J. Theor. Phys.* **38**, 1113 (1999)
 - [8] S. S. Gubser, *Phys. Rev. D* **78** (2008) 065034
 - [9] S. A. Hartnoll, C. P. Herzog and G. T. Horowitz, *Phys. Rev. Lett.* **101**, 031601 (2008)
 - [10] S. A. Hartnoll, C. P. Herzog and G. T. Horowitz, *JHEP* **0812** (2008) 015
 - [11] Y. B. Zel'dovich, *Zh. Eksp. Teor. Fiz* **62** (1972) 2076
 - [12] A. Starobinski, *Zh. Eksp. Teor. Fiz.* **64** (1973) 48.

- [13] T. Damour, N. Deruelle and R. Ruffini, Lett. Nuovo Ci- mento 15, 257 (1976).
- [14] H. Yoshino and H. Kodama, Prog. Theor. Phys. **128** (2012) 153
- [15] S. W. Hawking and H. S. Reall, Phys. Rev. D **61**, 024014 (2000)
- [16] W. H. Press and S. A. Teukolsky, Nature 238 (1972) 211212
- [17] V. Cardoso, O. J. C. Dias, J. P. S. Lemos and S. Yoshida, Phys. Rev. D **70** (2004) 044039
- [18] J. D. Bekenstein, Phys. Rev. D **7**, 949 (1973).
- [19] N. Uchikata and S. Yoshida, Phys. Rev. D **83**, 064020 (2011)
- [20] O. J. C. Dias and R. Masachs, JHEP **1702**, 128 (2017)
- [21] P. Breitenlohner and D.Z. Freedman, Phys. Lett. 115 B, 197 (1982).
- [22] P. Breitenlohner and D.Z. Freedman, Ann. Phys. 144, 249-281 (1982).
- [23] N. Iizuka, A. Ishibashi and K. Maeda, JHEP **1508**, 112 (2015)
- [24] C. Dappiaggi, H. R. C. Ferreira and C. A. R. Herdeiro, Phys. Lett. B **778**, 146 (2018)
- [25] A. Ishibashi and A. Hosoya, Phys. Rev. D **60**, 104028 (1999)
- [26] E. Witten, hep-th/0112258.
- [27] F. Olver, *NIST Handbook of Mathematical Functions*, Cambridge University Press (2010).
- [28] G. Denardo and R. Ruffini, Phys. Lett. **45B**, 259 (1973).
- [29] V. Cardoso and O. J. C. Dias, Phys. Rev. D **70**, 084011 (2004)
- [30] V. Cardoso, O. J. C. Dias and S. Yoshida, Phys. Rev. D **74**, 044008 (2006)
- [31] R. Brito, V. Cardoso and P. Pani, Lect. Notes Phys. **906**, pp.1 (2015)
- [32] M. Reed and B. Simon, Fourier Analysis, Self-Adjointness, (Academic Press, New York, 1975).
- [33] R.M. Wald, *General Relativity* (University of Chicago Press, Chicago, 1984).
- [34] A. Ishibashi, private communication.